# Chapter 4
# From Orbital Models to Accurate Predictions

**Abstract** Basic understanding and qualitative prediction of the isotropic magnetic coupling between two magnetic centers can be obtained with two well-established valence-only models. This chapter discusses the Kahn–Briat and Hay–Thibeault–Hoffmann models, which have been (and still are) of fundamental importance for understanding the basics of magnetism in polynuclear transition metal complexes. After shortly presenting the basic model for magnetism in organic radicals, we review the most evident magnetostructural relations and then move to the accurate prediction of the magnetic coupling. An overview of the most widely used quantum chemical methods is given, including wave function based methods and approaches within the spin-unrestricted setting such as density functional theory. The last part of the chapter is dedicated to the calculation of the interactions beyond the isotropic magnetic coupling.

## 4.1 Qualitative Valence-Only Models

The simplest electronic structure models for magnetic interactions only consider the unpaired electrons and their orbitals. All other electrons are taken as inactive and not included in the description. This leads to very simple wave functions, especially in the case of two identical $S = \frac{1}{2}$ magnetic centers. Such valence-only models, where *valence* is not used in its usual chemical context, are numerically not competitive with large-scale all-electron calculations, but have provided chemists and other scientists working in the field with important insights to control the magnetic interactions in transition metal complexes and materials with organic radicals.

### *4.1.1 The Kahn–Briat Model*

Based on valence bond reasoning with nonorthogonal atomic-like orbitals, Kahn and Briat derived an elegant model that is capable of explaining and predicting magnetic behavior of transition metal complexes based on the shape of the localized magnetic

© Springer International Publishing Switzerland 2016

C. Graaf and R. Broer, *Magnetic Interactions in Molecules and Solids*,
Theoretical Chemistry and Computational Modelling,
DOI 10.1007/978-3-319-22951-5_4

orbitals [1]. Let $\phi_a$ and $\phi_b$ be the optimal local orbitals for the unpaired electrons on site $A$ and $B$. These orbitals are normalized but not orthogonal

$$\langle\phi_a|\phi_b\rangle = S \qquad \langle\phi_a|\phi_a\rangle = \langle\phi_b|\phi_b\rangle = 1 \tag{4.1}$$

Multiplying the spatial part of the wave function $|\phi_a\phi_b| = |ab|$ with the singlet and triplet ($M_S = 0$) spin functions, the following normalized wave functions are obtained

$$\Psi_S = \frac{|a\overline{b}| + |b\overline{a}|}{\sqrt{2+2S^2}} \qquad \Psi_T = \frac{|a\overline{b}| - |b\overline{a}|}{\sqrt{2-2S^2}} \tag{4.2}$$

**4.1** Confirm that the norms of $\Psi_S$ and $\Psi_T$ are equal to 1.

As shown in the previous chapter, the energy difference between singlet and triplet is proportional to the magnetic coupling strength. The energy expectation values of $\Psi_S$ and $\Psi_T$ are

$$E_{S,T} = \frac{\langle a\overline{b} \pm b\overline{a}|\hat{H}|a\overline{b} \pm b\overline{a}\rangle}{\langle a\overline{b} \pm b\overline{a}|a\overline{b} \pm b\overline{a}\rangle} = \frac{\langle a\overline{b} \pm b\overline{a}|\hat{H}|a\overline{b} \pm b\overline{a}\rangle}{2 \pm 2S} \tag{4.3}$$

with

$$\hat{H} = \hat{h}_1(1) + \hat{h}_1(2) + \frac{1-\hat{P}_{12}}{r_{12}} \tag{4.4}$$

where $\hat{P}_{12}$ is the permutation operator. To avoid lengthy equations, some parameters will be introduced to facilitate the derivation.

$$\varepsilon = \langle a|\hat{h}_1|a\rangle = \langle b|\hat{h}_1|b\rangle \tag{4.5a}$$

$$\beta = \langle a|\hat{h}_1|b\rangle = \langle b|\hat{h}_1|a\rangle \tag{4.5b}$$

$$J^C = \langle ab|\frac{1}{r_{12}}|ab\rangle \tag{4.5c}$$

$$K = \langle ab|\frac{1}{r_{12}}|ba\rangle \tag{4.5d}$$

This results in the following expressions for the energy of the singlet and triplet states.

$$E_S = \frac{4\varepsilon + 4\beta S + 2J^C + 2K}{2 + 2S^2} = \frac{2\varepsilon + 2\beta S + J^C + K}{1 + S^2} \tag{4.6a}$$

$$E_T = \frac{4\varepsilon - 4\beta S + 2J^C - 2K}{2 - 2S^2} = \frac{2\varepsilon - 2\beta S + J^C - K}{1 - S^2} \tag{4.6b}$$

The energy difference is

$$\begin{aligned} E_S - E_T &= \frac{(2\varepsilon + 2\beta S + J^C + K)(1 - S^2)}{(1 + S^2)(1 - S^2)} - \frac{(2\varepsilon - 2\beta S + J^C - K)(1 + S^2)}{(1 - S^2)(1 + S^2)} \\ &= \frac{4\beta S + 2K - 4\varepsilon S^2 - 2J^C S^2}{1 - S^4} \end{aligned} \tag{4.7}$$

In general the overlap between the orbitals $a$ and $b$ is rather small given the fact that the magnetic centers are separated in space. Hence, the $S^4$ term can safely be discarded, and often the terms that are quadratic in the overlap are also neglected.

$$E_S - E_T \approx 2K - 4\varepsilon S^2 + 4\beta S - 2J^C S^2 \tag{4.8}$$

$$\approx 2K + 4\beta S \tag{4.9}$$

The second equation is the basis of the Kahn–Briat model. Given that $K$ is positive and $S$ opposite in sign to $\beta$, the energy difference between singlet and triplet can be interpreted as the sum of two opposite contributions. The direct exchange interaction between the electrons on both magnetic sites is dominant in case of negligible or zero overlap, for example due to different symmetries of the orbitals $a$ and $b$. This favors a ferromagnetic alignment of the spin moments, while a large overlap between the magnetic orbitals favors the singlet, and hence, enhances the antiferromagnetic character of the coupling.

The generalization to two magnetic centers with more than one unpaired electron can be made by the introduction of *exchange pathways*. The total magnetic coupling parameter $J$ of the Heisenberg Hamiltonian is decomposed as a sum of all the possible pairwise interactions weighted by the product of the number of unpaired electrons

$$J = \frac{1}{n_a n_b} \sum_{i \in A} \sum_{j \in B} J_{ij} \tag{4.10}$$

where each $J_{ij}$ is evaluated with the equation derived for two unpaired electrons (Eq. 4.9) and $n_a$ and $n_b$ make reference to the number of the unpaired electrons on the magnetic centers $A$ and $B$.

### 4.1.2 The Hay–Thibeault–Hoffmann Model

The second valence-only model starts from a molecular orbital viewpoint and was derived in the mid 1970s by Hay, Thibeault and Hoffmann (HTH) [2], approximately at the same time as the Kahn–Briat model. The magnetic orbitals are defined as linear combinations of orthogonal atomic-like orbitals

$$\phi_1 = \frac{1}{\sqrt{2}}(\psi_a + \psi_b) \qquad \phi_2 = \frac{1}{\sqrt{2}}(\psi_a - \psi_b) \tag{4.11}$$

Similar to $\phi_a$ and $\phi_b$ of the Kahn–Briat model, the atomic-like orbitals of the HTH model have the largest amplitudes on the magnetic centers, but in contrast $\psi_a$ and $\psi_b$ show delocalization tails on the ligands to ensure the orthogonality between them. Therefore, in general $\psi_a$ and $\psi_b$ are slightly more delocalized than the nonorthogonal $\phi_a$ and $\phi_b$.

In the original derivation, three determinants were constructed with the molecular orbitals $\phi_1$ and $\phi_2$

$$T = |\phi_1\phi_2| \qquad S_1 = |\phi_1\overline{\phi_1}| \qquad S_2 = |\phi_2\overline{\phi_2}| \tag{4.12}$$

with the following energy expectation values

$$\begin{aligned} E_T &= \langle\phi_1|\hat{h}_1|\phi_1\rangle + \langle\phi_2|\hat{h}_1|\phi_2\rangle + \langle\phi_1\phi_2|\frac{1}{r_{12}}|\phi_1\phi_2\rangle - \langle\phi_1\phi_2|\frac{1}{r_{12}}|\phi_2\phi_1\rangle \\ &= h_1 + h_2 + J_{12} - K_{12} \\ E_{S_1} &= 2\langle\phi_1|\hat{h}_1|\phi_1\rangle + \langle\phi_1\phi_1|\frac{1}{r_{12}}|\phi_1\phi_1\rangle = 2h_1 + J_{11} \\ E_{S_2} &= 2\langle\phi_2|\hat{h}_1|\phi_2\rangle + \langle\phi_2\phi_2|\frac{1}{r_{12}}|\phi_2\phi_2\rangle = 2h_2 + J_{22} \end{aligned} \tag{4.13}$$

$S_1$ and $S_2$ have the same spin and spatial symmetry and to obtain the energy of the lowest singlet a $2 \times 2$ matrix has to be diagonalized with $E_{S_1}$ and $E_{S_2}$ on the diagonal and the interaction between the two determinants as off-diagonal element

$$\langle S_1|\hat{H}|S_2\rangle = \langle\phi_1\phi_1|\frac{1}{r_{12}}|\phi_2\phi_2\rangle = \langle\phi_1\phi_2|\frac{1}{r_{12}}|\phi_2\phi_1\rangle = K_{12} \tag{4.14}$$

The second-order equation that arises from the condition that the secular determinant is equal to zero can be solved straightforwardly and gives the energy of the singlet

$$E_S = h_1 + h_2 + \frac{1}{2}(J_{11} + J_{22}) - \frac{1}{2}\sqrt{(2h_1 - 2h_2 + J_{11} - J_{22})^2 + 4K_{12}^2} \tag{4.15}$$

and the energy difference between singlet and triplet becomes

$$E_S - E_T = \frac{1}{2}(J_{11} + J_{22}) - \frac{1}{2}\sqrt{(2h_1 - 2h_2 + J_{11} - J_{22})^2 + 4K_{12}^2} - J_{12} + K_{12} \quad (4.16)$$

The square root term in the difference can be simplified by assuming that $J_{11} - J_{22}$ is small and that $4K_{12}^2$ is significantly larger than $(h_1 - h_2)^2$. The term then reduces to

$$\begin{aligned}\sqrt{(2h_1 - 2h_2 + J_{11} - J_{22})^2 + 4K_{12}^2} &\approx \sqrt{(2h_1 - 2h_2)^2 + 4K_{12}^2} \\ &\approx 2K_{12} + \frac{(h_1 - h_2)^2}{K_{12}} \end{aligned} \quad (4.17)$$

using the Taylor series $\sqrt{p+q} = \sqrt{p} + \frac{1}{2}q/\sqrt{p} + \ldots$ with $p \gg q$. The expression for the energy difference now reads

$$E_S - E_T = \frac{1}{2}(J_{11} + J_{22}) - \frac{(h_1 - h_2)^2}{2K_{12}} - J_{12} \quad (4.18)$$

which is further simplified by introducing the orbital energies of the magnetic orbitals, which for the triplet state are defined as

$$\varepsilon_1 = h_1 + J_{12} - K_{12} \qquad \varepsilon_2 = h_2 + J_{12} - K_{12} \quad (4.19)$$

and makes that $h_1 - h_2$ can be replaced by $\varepsilon_1 - \varepsilon_2$, which is a much easier quantity to work with. The expression shows that in the HTH model the magnetic coupling can be obtained from the outcomes of one single restricted Hartree–Fock (RHF) calculation for the triplet state. Furthermore, by expressing the integrals using the local orbitals $\psi_a$ and $\psi_b$ instead of the molecular orbitals $\phi_1$ and $\phi_2$, the expression can be written even more compact. Through a somewhat tedious but straightforward derivation it can be shown that

$$\begin{aligned} J_{11} &= \frac{1}{2}(J_{aa} + J_{ab}) + K_{ab} + 2\langle aa|\frac{1}{r_{12}}|ab\rangle \\ J_{22} &= \frac{1}{2}(J_{aa} + J_{ab}) + K_{ab} - 2\langle aa|\frac{1}{r_{12}}|ab\rangle \\ J_{12} &= \frac{1}{2}(J_{aa} + J_{ab}) - K_{ab} \\ K_{12} &= \frac{1}{2}(J_{aa} - J_{ab}) \end{aligned} \quad (4.20)$$

**4.2** Use the definitions of $\phi_1$ and $\phi_2$ given in Eq. 4.11 to express the integral $J_{11}$ in terms of local orbitals. Remember that $\int \phi_a(1)\phi_a(2)(1/r_{12})\phi_b(1)\phi_b(2)d\tau = \int \phi_a(1)\phi_b(1)(1/r_{12})\phi_a(2)\phi_b(2)d\tau = K_{ab}$.

This brings us to the final expression of the HTH model for the singlet-triplet splitting

$$E_S - E_T = 2K_{ab} - \frac{(\varepsilon_1 - \varepsilon_2)^2}{J_{aa} - J_{ab}} \tag{4.21}$$

where immediately the two opposite contributions to the magnetic coupling can be recognized. The direct exchange $K_{ab}$ favors the triplet, and hence, the parallel alignment of the spin moments. On the other hand, a large splitting between the orbital energies of $\phi_1$ and $\phi_2$ favors the antiferromagnetic component of the coupling $J_{aa} > J_{ab}$.

The magnetic coupling in systems with $m$ unpaired electrons per magnetic center can also be studied with the HTH model. The direct exchange is written as the sum of exchange integrals between orbitals on center $A$ and center $B$

$$K = \sum_{i \in A} \sum_{j \in B} K_{ij} \tag{4.22}$$

To evaluate the antiferromagnetic part of the coupling, the magnetic orbitals are grouped in pairs of *bonding* and *antibonding* orbitals and the total contribution is defined as the sum of the individual couplings divided by $m^2$

$$J^{AF} = -\frac{1}{m^2} \sum_{i=1}^{m/2} \frac{(\varepsilon_i - \varepsilon_{2i})^2}{J_{a_i a_i} - J_{a_i b_i}} \tag{4.23}$$

where $\varepsilon_i$ is the orbital energy of the binding combination of $\psi_a$ and $\psi_b$, and $\varepsilon_{2i}$ the orbital energy of the antibonding combination.

### *4.1.3 McConnell's Model*

The valence-only models discussed so far have been developed in the field of transition metal compounds, either molecular based or in extended systems. The dominant magnetic interactions in these systems typically involve atoms that are bonded through bridging diamagnetic ligands, the so-called through-bond interactions. In magnetic materials based on organic radicals the mechanism is fundamentally different; there is no diamagnetic bridge between the magnetic centers and the description of the interaction given in Sect. 3.1 (and further analyzed in Chap. 5) does not

directly apply. Traditionally the magnetism caused by through-space interactions in such organic materials is rationalized with the McConnell I model [3]. To describe the interaction between two radicals, the model takes an atomic viewpoint and starts with the Heisenberg Hamiltonian in the following form

$$\hat{H} = -\sum_{i<j} J_{ij}\hat{S}_i\hat{S}_j \tag{4.24}$$

where the sum runs over all the atoms in the two radicals. The $J_{ij}$ parameters can be interpreted as the parameter for the coupling of an electron in atomic orbital $\phi_i$ on site $i$ and another electron in $\phi_j$ on site $j$. In a valence bond setting with non-orthogonal orbitals, the interaction can be written as the sum of a positive two-electron exchange integral and a one-electron integral

$$J_{ij} = \langle\phi_i\phi_j|\frac{1}{r_{12}}|\phi_j\phi_i\rangle + \langle\phi_i|\phi_j\rangle\langle\phi_i|\hat{h}(1)|\phi_j\rangle \tag{4.25}$$

The one-electron integral is dominated by the electron-nucleus attraction in most cases, and hence, negative in sign. From this it is concluded that, unless the overlap between the orbitals $\phi_i$ and $\phi_j$ is very small, the $J_{ij}$ parameter is negative, favoring singlet coupling of the electrons. This expression is not very easy to handle and in all practical applications to rationalize the magnetic properties of radicals a series of simplifications is introduced. In the first place the summation is restricted to pairs of electrons on different units

$$\hat{H} = -\sum_{i\in A}\sum_{j\in B} J_{ij}\hat{S}_i\hat{S}_j \tag{4.26}$$

assuming that the interactions within a unit do not depend on the coupling of the total spin moment of the two radicals. The second and most fundamental approximation of McConnell's model is made by replacing the spin operators by a product of the total spin operator for each unit and the atomic spin populations $\rho_i$

$$\hat{H} = -\hat{S}_A \cdot \hat{S}_B \sum_{i\in A}\sum_{j\in B} J_{ij}\rho_i\rho_j \tag{4.27}$$

The third simplification lies in the restriction of the sum over $i$ and $j$ to the shortest contacts only. Thus, second nearest neighbour interactions (and beyond) between the units, which in many cases oppose the nearest neighbour interactions, are neglected. These simplifications lead to a very simple model to rationalize or predict magnetic properties of molecular crystals based on organic radicals. When regions of opposite spin densities overlap, $\rho_i\rho_j < 0$ one can expect ferromagnetic interactions and when close contacts have spin populations with the same sign, $\rho_i\rho_j > 0$, antiferromagnetism prevails. To illustrate its application, we consider two stacked benzyl radicals with the $CH_2$ groups in *para* and *meta* as illustrated in Fig. 4.1. The spin populations

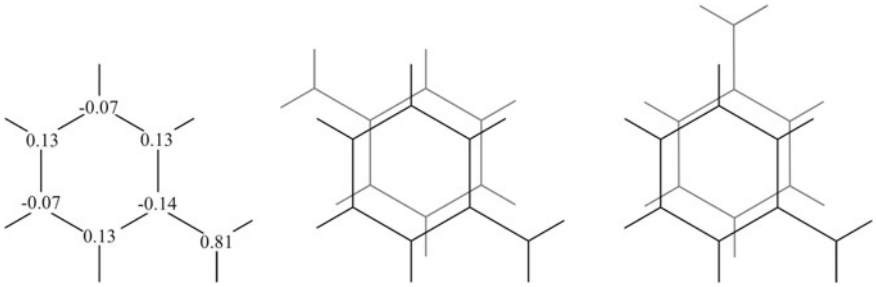


**Fig. 4.1** *Left* Benzyl radical with the spin populations of the carbon atoms. Two benzyl radicals stacked with the $CH_2$ group in *para* (*middle*) and *meta* position (*right*)

shown in the left part of the figure have been calculated with a simple CASSCF calculation on the doublet spin state of the monomer, although in this case the alternation of the sign of the spin population can be anticipated. The closest contacts in the stacked dimers are formed by the aligned carbon atoms of the benzene ring. The $\rho_i \rho_j$ products for these atoms are all negative in the case of the *para* conformer (middle of Fig. 4.1) and therefore this dimer is expected to have a triplet ground state. The aligned carbon atoms of the *meta* conformer (right) have spin populations of the same sign, the $\rho_i \rho_j$ product is therefore positive, predicting an antiferromagnetic (singlet) ground state.

The conclusions on the nature of the ground state in the benzyl dimer extracted from the model of McConnell are in line with those of accurate ab initio calculations. Also in many organic magnetic materials, the model has proven its ability to correctly reproduce the dominant magnetic interactions. However, the careful step-by-step analysis of the model by Novoa and co-workers [4, 5] showed that the success of the model is at least partially due to a fortunate cancellation of errors. The analysis shows that there is no firm theoretical foundation for replacing the spin operators by atomic spin densities. Moreover, the model was shown to fail to predict the dominant magnetic interactions in several crystals with nitronyl nitroxide radicals and cannot reproduce the angle dependence of the magnetic interaction in the model system containing two $H_2NO$ radicals. Hence, despite its numerous successes and versatility, the McConnell model should be applied with caution.

**4.3** Use the reasoning of McConnell's model (Eq. 4.27) to predict the ground state of the benzyl dimer with the $CH_2$ groups in *ortho* and for the conformer where the two units are perfectly aligned.

## 4.2 Magnetostructural Correlations

From the very beginning of the study of the magnetic interactions in transition metal complexes a large part of the effort has been dedicated to derive relations between the geometrical structure of the complex and the nature and magnitude of the coupling of the localized spin moments. These magnetostructural correlations can be extremely useful to rationalize the variations in the magnetic behaviour of a family of similar complexes or to design new complexes with the desired properties. Magnetostructural relations can be extracted from experimental studies by comparing a large group of compounds and relate geometric parameters with the observed magnetic behaviour. This requires a large set of data, but it is often difficult to separate different (opposing) effects. On the other hand, theoretical studies can take a (model) complex and modify the geometry at will to establish the influence of a certain geometric parameter on the magnetic interaction. Combined with the qualitative valence-only models discussed in the previous sections one can boil down the complicated magnetic behaviour to very simple concepts and straightforward magnetostructural correlations. These concepts and correlations can yield design rules that can be utilized in the synthesis of materials with pre-defined magnetic properties.

**M–L–M angle**: One of the most famous magnetostructural correlations concerns the dependence of $J$ on the M–L–M angle in transition metal complexes with a double bridge as depicted in Fig. 3.1. For angles close to 90° the coupling of the spin moments on the metal ions is ferromagnetic and for larger (and smaller) angles the coupling becomes antiferromagnetic. The curve shown in Fig. 4.2 is a typical example of this correlation and was obtained by calculating $J$ from the singlet-triplet energy difference (see Eq. 3.29) using the wave functions discussed in Sect. 3.1, Eqs. 3.2a and 3.7. The change from ferromagnetic to antiferromagnetic interaction can be explained with the Hay–Thibeault–Hoffmann model. The largest contributions to

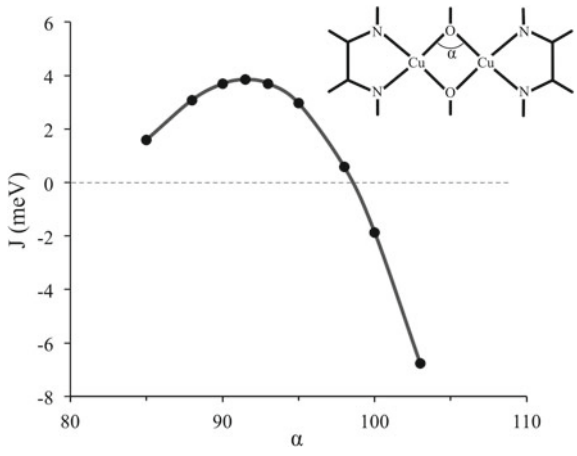


**Fig. 4.2** Magnetic coupling strength of the copper dimer shown in the inset versus the angle $\alpha$

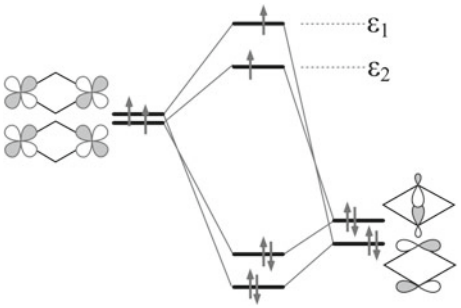


**Fig. 4.3** Molecular orbital diagram showing the interaction of the plus and minus combinations of the $3d_{xy}$ orbitals on the metal centers with the $p_x$ and $p_y$ orbitals on the ligands

the magnetic orbitals arise from the plus and minus combinations of the Cu-$3d_{xy}$ orbitals, shown on the left in Fig. 4.3. The plus and minus combinations of the $p_x$ and $p_y$ orbitals on the bridge in the right column of the MO diagram interact with the $3d_{xy}$ orbitals to form bonding and antibonding combinations as shown in the middle of the figure. The bonding orbitals are doubly occupied and not relevant for the magnetic properties, but the antibonding combinations correspond to the magnetic orbitals, in which we readily recognize the large contribution from the $3d_{xy}$ orbitals with non-negligible tails on the ligand. In the reasoning of the HTH model, the difference in orbital energy $\varepsilon$ of the two magnetic orbitals is directly related to the magnetic coupling strength, cf. Eq. 4.21 and numerically proven by Ruiz and co-workers in Ref. [6]. For (nearly) degenerate magnetic orbitals ($\varepsilon_1 \approx \varepsilon_2$) the antiferromagnetic term is small and the direct exchange $K_{ab}$ dominates. However, when the orbital energies are sufficiently different, the antiferromagnetic term is the largest term and $J$ will become negative.

The upper part of Fig. 4.4 shows that the interaction of the $p_x$ and $p_y$ bridge orbitals with the $3d_{xy}$ orbitals on the metal is approximately equal around $\alpha = 90°$. Therefore, the near degeneracy of the plus and minus combination of the 3d orbitals is maintained and one can expect a small ferromagnetic interaction of the spins. On the contrary, for larger angles, the interaction along the $x$-direction becomes stronger than for the $y$ orbitals. This is reflected in a larger delocalization onto the ligand in the *gerade* orbital than in the *ungerade* orbital,[1] see the lower part of Fig. 4.4. The energies of the two magnetic orbitals are no longer similar and a considerable antiferromagnetic contribution exists, which for large enough angles overcomes the ferromagnetic contribution and turns the net coupling in an antiferromagnetic one.

**Out-of plane angle**: A second interesting magnetostructural relation that can easily be explained with the HTH model is the increase in ferromagnetic coupling when the side group of the bridging atoms is rotated out of the M–$(L)_2$–M plane. This relation was described in detail in Ref. [6] and it was found that ferromagnetic coupling can be obtained even in those molecules that have a rather large M–L–M angle. Figure 4.5

[1] *Gerade* and *ungerade* (odd and even in German) make reference to the effect of the sign of the orbital under the action of the inversion operator. The *gerade* orbital does not change sign, while the *ungerade* orbital is converted to its opposite.

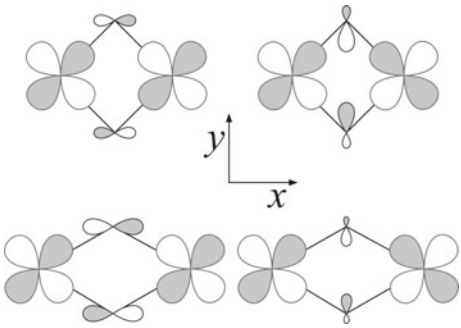


**Fig. 4.4** *Upper part gerade* and *ungerade* magnetic molecular orbitals for a M–L–M angle of 90°. The $d_{xy}$ orbitals on the metal centers have an equal overlap with the $p_x$ and $p_y$ orbitals on the ligand. *Lower part* In a system with a larger M–L–M angle, the overlap is larger for $p_x$ than for $p_y$

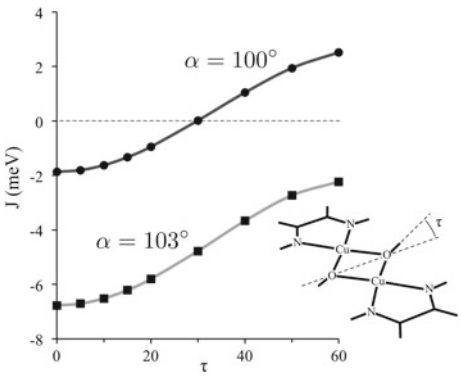


**Fig. 4.5** Magnetic coupling strength $J = E_S - E_T$ as function of the out-of-plane angle $\tau$ for two different Cu–O–Cu angles

shows how the magnetic coupling varies when the hydrogen atom of the bridging OH groups is moved out of the plane formed by the Cu and O ions. In the case of the 103° Cu–O–Cu angle (squares), the magnetic coupling is diminished by approximately 4.5 meV but the ferromagnetic regime is not reached. Considering a slightly smaller M–L–M angle (circles), a similar change in the coupling is observed but now the behaviour is changed from antiferromagnetic to ferromagnetic near $\tau = 30°$.

The increased ferromagnetic character of the coupling upon the out-of-plane movement of the side group of the bridging ligand (in this simple case a hydrogen atom, but the same tendency is observed for bigger residues) is easily explained with the MO diagram represented in Fig. 4.3. In the case of a completely flat magnetic core, that is $\tau = 0°$, the ligand orbital in the $xy$-plane oriented along the $y$-axis ($\phi_1$) is typically composed of $sp$ hybrids, mixtures of $s$ and $p_y$ orbitals. When $\tau$ is different from zero, the $xy$-plane is no longer a symmetry plane of the complex and the $p_z$ orbitals can also contribute to $\phi_1$. This means that the hybridization is no longer purely $sp$, but has also some $sp^2$ character. The increased $p$-character of the hybrid increases the ligand orbital energy and reduces the gap with the $3d_{xy}$ orbitals in the left of Fig. 4.3. Consequently, the interaction becomes stronger and the antibonding combination, the magnetic orbital with energy $\varepsilon_2$, will be higher in energy. This reduces $(\varepsilon_1 - \varepsilon_2)^2$ and weakens the antiferromagnetic contribution to the coupling.

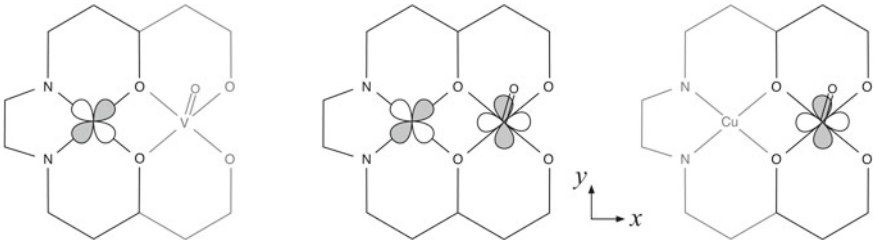


**Fig. 4.6** Schematic representation of the Cu/V binuclear complex with a double alkoxo bridge. *Left* and *right* Magnetic orbitals for the Cu site and the V site, respectively. *Middle* superposition of the two magnetic orbitals

**Exchange pathways**: We will now further expand the relation between geometry and magnetic coupling strength by exploiting the concept of the *exchange pathway*, which was already briefly mentioned at the end of Sect. 4.1.1. For systems with more than one unpaired electron per magnetic center the Kahn–Briat model decomposes the total coupling in pairwise contributions as given in Eq. 4.10. These exchange pathways provide a very powerful tool to predict the nature of the magnetic coupling (ferro- or antiferromagnetic; weak, strong) in nearly all combinations of $d^n$ magnetic ions. Many examples were discussed in the book by Kahn [7] and the concept has recently been reviewed by Launay and Verdaguer [8]. Here we will shortly discuss two examples to clarify the way of reasoning to rationalize or predict the nature of the coupling between two transition metals bridged by one or more diamagnetic ligands. For a full account on this subject we refer to the books of Kahn, and Launay and Verdaguer.

The first step in the procedure consist of an inspection of the coordination sphere of the magnetic centers to determine the shape and symmetry of the optimal local magnetic orbitals. This can either be done through calculation or by ligand field reasoning. Our first example is a binuclear complex of $Cu^{2+}$ and $V^{4+}$ with a double alkoxo-bridge. The copper ion has a $d^9$ electronic configuration. This means that all $3d$-orbitals are doubly occupied except the $3d_{xy}$ orbital, which is highest in energy because it directly points to the atoms of the first coordination sphere. The vanadium ion is covalently bound to the apex oxygen and the resulting vanadyl group has a formal oxidation state of VO(II) with one unpaired electron in the orbital of lowest energy, the largely non-bonding V-$3d_{x^2-y^2}$ orbital. Figure 4.6 shows the two magnetic orbitals of the two magnetic centers, the left panel corresponds to the magnetic orbital on Cu and the right panel to the VO site. The superposition of these two pictures in the middle defines the exchange pathway and can help us to decide upon the overlap between the two orbitals as they appear in the main equation of the Kahn–Briat model, see Eq. 4.9. Note, that this does not define a molecular orbital, it is merely a construction by superimposing the two magnetic orbitals. The product of the two functions is an odd function with respect to the $xz$-plane, and hence, integrating over the cartesian coordinates gives a zero overlap integral $S$ of these two magnetic orbitals. When $S$ is equal or close to zero, the first term in the Kahn–Briat equation determines

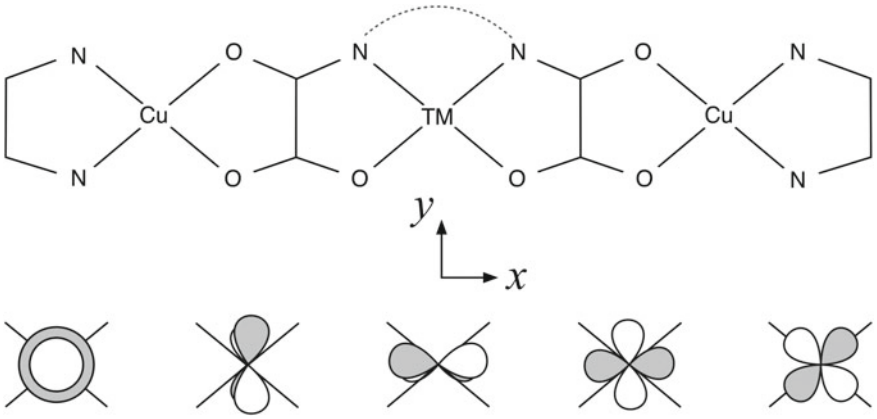


**Fig. 4.7** Trinuclear model complex with $C_{2v}$ symmetry. TM is one of the transition metals with an incomplete $d^n$ electronic configuration with high spin coupling. The orbitals in the lower part are $3d_{z^2}$ ($a_1$), $3d_{yz}$ ($b_2$), $3d_{xz}$ ($b_1$), $3d_{x^2-y^2}$ ($a_1$) and $3d_{xy}$ ($a_2$) and are ordered from *left* to *right* by increasing orbital energy

the nature of the coupling. Therefore, the magnetic coupling in this Cu/V dimer is expected to be ferromagnetic, in line with the triplet ground state and singlet-triplet gap of approximately $100\,\mathrm{cm}^{-1}$ observed experimentally [9].

In complexes with more than one unpaired electron on at least one of the magnetic sites, the overall magnetic coupling is the sum of the couplings along all exchange paths weighted by the product of the number of unpaired electrons on each magnetic center (the number of paths). To illustrate the potential of the Kahn–Briat model for predicting the nature of the magnetic coupling, we will focus on the trinuclear $Cu^{II}$ complex schematically depicted in the upper part of Fig. 4.7 and discuss the effect of replacing the copper ion in the middle by other transition metals. The complex has approximate $C_{2v}$ symmetry and the five $3d$ orbitals belong to the $a_1$ (2x), $a_2$, $b_1$ and $b_2$ irreducible representations as shown in the lower part of the figure. The copper ions on the left and right sides of the complex with their $3d^9$ electronic configuration have only one unpaired electron, which resides in the $3d_{xy}$ orbital of $a_2$ symmetry. When the magnetic center in the middle is also occupied by a $Cu^{2+}$ ion, the three magnetic orbitals are all of the same symmetry and hence there is a non-zero overlap leading to an antiferromagnetic coupling between the TM ions in the complex, in line with experiment [10].

Keeping track of the relative energy of the five $3d$ orbitals (see Fig. 4.7), we now consider the complexes that contain transition metals with other electronic configurations. Starting with the $3d^1$ configuration (for example, $Ti^{3+}$), the natural magnetic orbital in the middle is $3d_{z^2}$ with $a_1$ symmetry and the Cu orbitals on the outside are $3d_{xy}$ of $a_2$ symmetry. Hence, the exchange path includes orthogonal orbitals and ferromagnetic interactions are expected. Putting a transition metal with two $d$-electrons in the middle leads to an electronic configuration with the unpaired electrons in the

$3d_{z^2}$ and $3d_{yz}$ orbitals belonging to the $a_1$ and $b_2$ irreducible representations, respectively. The total coupling is a sum of four exchange paths, which appear in two pairs because of the left–right symmetry of the complex. Exchange path type 1 goes from the $3d_{z^2}$ orbital in the middle to the $3d_{xy}$ orbital on the Cu. Since they transform differently under the symmetry operations of the $C_{2v}$ group, the overlap integral of the two orbitals is zero and this path contributes in a ferromagnetic way to the coupling. The same holds for the second pair of exchange paths involving the $3d_{yz}$ and $3d_{xy}$ orbitals. Hence, again a ferromagnetic coupling can be anticipated. The situation changes when the middle position is occupied by an ion with a $d^5$ electronic configuration. Five different exchange paths are now active; four of them involve orthogonal orbitals, but the fifth connects the $3d_{xy}$ natural magnetic orbitals of the centers. The latter gives an antiferromagnetic contribution and counterbalances the four weaker ferromagnetic exchange paths. When TM ions are placed in the center with more than 5 $d$-electrons, the ferromagnetic exchange paths disappear, the coupling gets gradually more antiferromagnetic until we arrive again at the strong antiferromagnetic coupling in the case of three ions with $d^9$ electronic configurations.

**4.4** Consider the complex sketched in this box and predict the nature of the coupling when site A is occupied by $Ni^{2+}$ and site B by $Cr^{3+}$. The out of plane TM-ligand distances are larger than the in-plane distances.

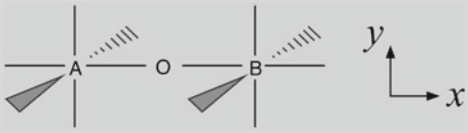


What is the number of exchange paths when $Cr^{3+}$ is replaced by $Mn^{2+}$? What coupling can be expeced?

**Counter-complementarity**: Another relation between structure and magnetic coupling strength is covered by the concept of counter-complementarity. In systems with two magnetic centers connected by two different ligands the total magnetic coupling is in general not equal to the sum of the magnetic coupling via the two individual bridges but often significantly smaller. This anti-synergistic effect can most efficiently be explained for a system with two $S = 1/2$ spin moments based on two molecular orbital diagrams using the HTH model. Figure 4.8 shows the interaction of the atomic-like orbitals on the magnetic centers $A$ and $B$ with those of the bridge ($L_1$) that is expected to give the largest contribution to the coupling. The molecule is in the $xy$-plane and the $A$–$B$ 'bond' is along the $x$-axis. The interaction of the $L_1 - p_x$ orbital with the *gerade* combination of $d_{xy}$ orbitals is stronger than the interaction of the $L_1 - 2p_y$ with the *ungerade* $d_{xy}$ orbitals. Therefore a gap is opened between the magnetic orbitals $\varphi_1$ and $\varphi_2$ with the antibonding combination of *gerade* $d_{xy}$ and $L_1 - 2p_x$ at higher energy. Equation 4.21 shows that this gap ($\Delta_1$) is directly proportional to the magnetic coupling through $L_1$.

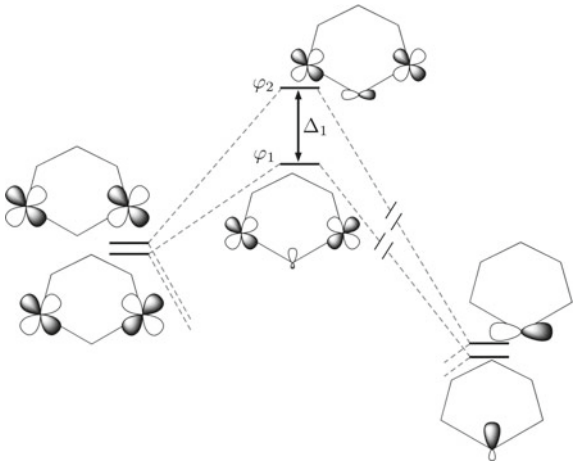


**Fig. 4.8** Molecular orbital diagram of the interaction of the atomic-like orbitals on the magnetic centers *A* and *B* and the orbitals on the lower bridge parallel and perpendicular to the *A*–*B* 'bond'

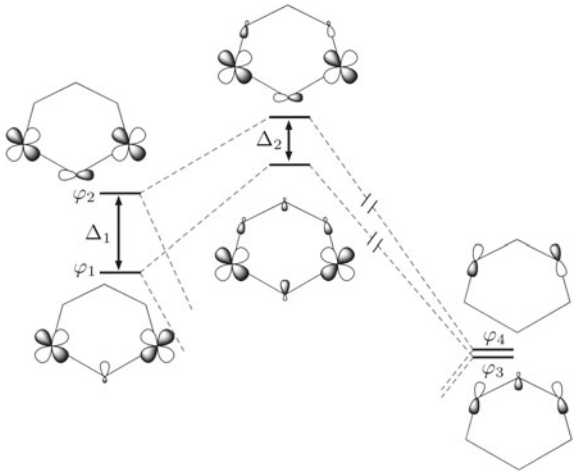


**Fig. 4.9** Molecular orbital diagram of the interaction of the magnetic orbitals $\varphi_1$ and $\varphi_2$ (obtained by the interaction of the magnetic centers with the lower bridge) and those of the upper ligand. $\Delta_1 > \Delta_2$

The next step takes into account the interaction with the second bridge ($L_2$) and is schematically depicted in Fig. 4.9. For symmetry reasons, $\varphi_1$ interacts with $\varphi_3$, and $\varphi_2$ with $\varphi_4$. If we take a perturbational point of view, the interaction strength is determined not only by the energy separation of the levels but also by the interaction matrix elements. The shape of the orbitals on the left and the right of the figure strongly suggest that the matrix elements can be assumed to be nearly the same, and hence, the final result of the interaction is solely determined by the differences in the orbital energies. $\varphi_3$ and $\varphi_4$ lie at lower energy than $\varphi_1$ and $\varphi_2$, but the separation between these two is much smaller than $\Delta_1$. From this directly follows that $\varepsilon(\varphi_1) - \varepsilon(\varphi_3)$ is smaller than $\varepsilon(\varphi_2) - \varepsilon(\varphi_4)$. Consequently, the destabilization in the antibonding combination of $\varphi_1$ and $\varphi_3$ is larger than for $\varphi_2$ and $\varphi_4$ and leads to a smaller gap between the magnetic orbitals than after the considering only $L_1$: $\Delta_1 > \Delta_2$.

According to the HTH model this gives a reduction of the antiferromagnetic contribution to the magnetic coupling (see Eq. 4.21) and illustrates the anti-synergistic effect or counter-complementarity of the two ligands.

## 4.3 Accurate Computational Models

Although the qualitative models discussed so far are very useful for a basic understanding of the magnetic interactions between two spin moments, more quantitative predictions can only be obtained by going beyond the *valence*-only description considered so far. As shown in the previous chapter, the magnetic interaction parameter $J$ of the Heisenberg Hamiltonian can in many cases be related to the energy difference of electronic states with different spin couplings. Hence, precise theoretical estimates of the magnetic coupling strengths are intimately related to the correct application of high-level computational schemes.

As shown in Sect. 3.1, the basic description of the magnetic coupling problem is intrinsically multideterminantal and in most cases one needs a multiconfigurational description for minimally accurate results. Before discussing the different computational schemes that can be used for quantitative estimates, we want to stress that a multideterminantal wave function is not necessarily a multiconfigurational wave function. This is best illustrated for the 2-electrons/2-orbitals case discussed before. The simplest representation of the triplet state is obtained with a single Slater determinant

$$\Phi_T = |\phi_a \phi_b| \tag{4.28}$$

where all the doubly occupied orbitals have been omitted. On the other hand, the most basic description of the open-shell singlet requires a wave function with two Slater determinants to fulfill the requirements of the spin symmetry.

$$\Phi_S = \frac{|\phi_a \overline{\phi}_b| - |\overline{\phi}_a \phi_b|}{\sqrt{2}} \tag{4.29}$$

This multideterminantal wave function only describes one electronic configuration since the occupation of the orbitals is the same in both determinants and is in general known as a configuration state function. In this simple monoconfigurational description, the energy of the triplet is lower than the singlet by twice the exchange integral $K_{ab}$. A more satisfactory description is obtained with a multiconfigurational singlet wave function by adding the Slater determinants with two electrons in the same orbital

$$\Phi'_S = c_1\{|\phi_a \overline{\phi}_b| - |\overline{\phi}_a \phi_b|\} + c_2\{|\phi_a \overline{\phi}_a| + |\phi_b \overline{\phi}_b|\} \tag{4.30}$$

where $c_1$ is much larger than $c_2$ for biradicalar systems, and their precise value has to be determined in a configuration interaction calculation. Wave functions of this

type are often used as multideterminantal-multiconfigurational reference—mostly multireference (MR), for short—wave function.

MR-CISD is one of the most accurate ab initio computational schemes that can be used to describe the electronic structure of systems with a markedly multireference character. Although the ever increasing computing power constantly pushes the frontiers forward, the applicability of MR-CISD remains limited to small (model) systems. Moreover, the method suffers from the size-extensivety problem inherent to any truncated CI method. For these reasons, MR-CISD is hardly ever used in computational studies of molecules with unpaired electrons. There are, however, several alternative wave function based schemes that can provide very useful information about the magnetic interactions. In the following sections we will first discuss the ins-and-outs of a good reference wave function and introduce the difference dedicated CI (DDCI) method. Thereafter a short account will be given of two implementations of MR perturbation theory, and the chapter will be closed with a discussion of the consequences of lifting the restrictions of the spin symmetry as done in density functional theory (DFT).

### *4.3.1 The Reference Wave Function and Excited Determinants*

An important factor in the accurate prediction of magnetic coupling (and other electronic structure) parameters is the proper choice of the reference wave function. There are many possible ways to construct the reference, but the complete active space (CAS) approach has emerged as one of the most versatile methods. The molecular orbitals are divided in three groups: the inactive, the active and the virtual orbitals. The orbitals in the first group are doubly occupied in all the Slater determinants of the multireference wave function, while the orbitals in the last group remain always unoccupied. The orbitals in the second class span the active space. The multiconfigurational wave function is generated by distributing $N_{act}$ electrons—where $N_{act}$ is the total number of electrons minus two times the number of inactive orbitals—over the $M_{act}$ active orbitals. This is schematically outlined in Fig. 4.10. The doubly occupied or empty Hartree Fock orbitals shown on the left are divided in inactive, active and virtual orbitals. The multiconfigurational wave function is constructed by making a linear combination of Slater determinants $\Phi_1$, $\Phi_2$, etc. that differ by the occupation of the active orbitals. The CAS procedure generates a MR wave function in which all possible distributions of the active electrons over the active orbitals are considered. Although this approach often generates many determinants that are very high in energy and are not specially important in the final wave function, it has several important practical and conceptual advantages like the good convergence properties, size extensivity, orbital invariance, etc. [11]. Moreover, it has the advantage that selecting the active orbital space (although far from being trivial) is in most cases easier than making an unbiased selection of the most important configurations.

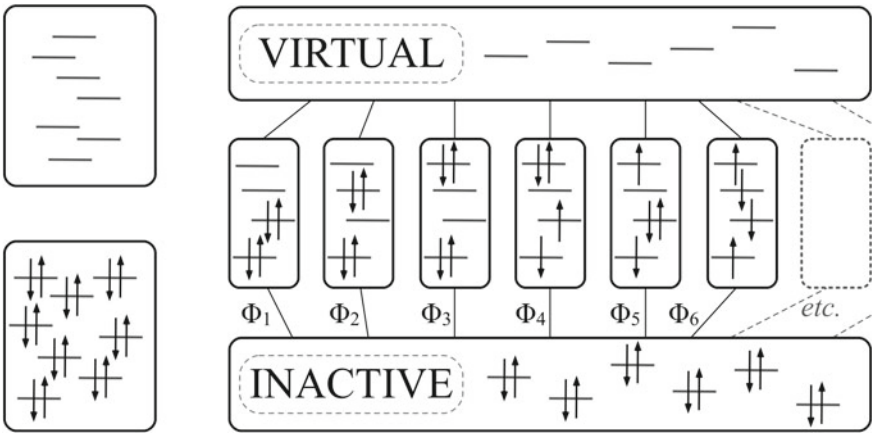


**Fig. 4.10** Complete Active Space procedure to generate a multireference wave function. The occupied and virtual orbitals from a Hartree–Fock calculation (*left*) are divided in three groups (*right*): Inactive, active and virtual orbitals. A linear combination of Slater determinants is formed in which the inactive orbitals are always doubly occupied, the virtual orbitals are always empty and the active orbitals can be doubly occupied, singly occupied or unoccupied

**4.5** How many determinants with $M_S = 0$ can be generated for the active space with 4 active orbitals and 4 electrons as shown in Fig. 4.10.

In virtually all calculations of magnetic interactions or related electronic structure parameters, the wave function expansion is restricted to singly and doubly excited determinants with respect to the reference. These determinants are often classified in eight different groups depending on how many holes/particles are created in the inactive/virtual orbitals. This can be very useful to decompose the wave function in smaller contributions and in this way facilitate the analysis of the results. Table 4.1 overviews the different classes and lists the labels used in some post Hartree–Fock methods that will be described in the remainder of this chapter. In the Table we have used $\hat{E}_{rs}$ to define the excitation operator $\hat{a}_s^\dagger \hat{a}_r$, eliminating an electron in orbital $r$ and creating one in orbital $s$.

It is rather complicated to give generally applicable formulas for the number of determinants in each class, but rough estimates are rather easily calculated. Consider a system with $k$ inactive orbitals, $l$ virtual orbitals and $n$ determinants in the reference wave function, the number of electrons is even and we restrict ourselves to the $M_S = 0$ subspace without any further spin or spatial symmetry. The approximate number of $2h$-$2p$ replacements is given by the product of the number of ways in which 2 holes can be created in the inactive orbitals ($k^2$) and the ways in which two particles can be placed in the virtual orbitals ($l^2$) multiplied with the number of determinants in the

**Table 4.1** Classification of the singly and doubly excited determinants by the number of holes/particles created in the inactive ($h$, $h'$)/virtual ($p$, $p'$) orbitals

| Excitation operator(s) | CASPT2 | DDCI | NEVPT2 |
|---|---|---|---|
| $\hat{E}_{ha}$; $\hat{E}_{ha}\hat{E}_{bc}$ | Internal | 1$h$ | $\hat{V}_{h}^{+1}$ |
| $\hat{E}_{ha}\hat{E}_{h'b}$ | | 2$h$ | $\hat{V}_{hh'}^{+2}$ |
| $\hat{E}_{ap}$; $\hat{E}_{ap}\hat{E}_{bc}$ | Semi-internal | 1$p$ | $\hat{V}_{p}^{-1}$ |
| $\hat{E}_{hp}$; $\hat{E}_{hp}\hat{E}_{ab}$ | | 1$h$-1$p$ | $\hat{V}_{h,p}^{0}$ |
| $\hat{E}_{hp}\hat{E}_{h'a}$ | | 2$h$-1$p$ | $\hat{V}_{hh',p}^{+1}$ |
| $\hat{E}_{ap}\hat{E}_{bp'}$ | External | 2$p$ | $\hat{V}_{pp'}^{-2}$ |
| $\hat{E}_{hp}\hat{E}_{ap'}$ | | 1$h$-2$p$ | $\hat{V}_{h,pp'}^{-1}$ |
| $\hat{E}_{hp}\hat{E}_{h'p'}$ | | 2$h$-2$p$ | $\hat{V}_{hh',pp'}^{0}$ |

$a$, $b$ and $c$ are active orbitals. The nomenclature used in some post Hartree–Fock methods is also listed

reference wave function, that is $n \times k^2 l^2$. A similar reasoning can be used to estimate the number of excitations with 2$h$-1$p$ ($n \times k^2 l$), 1$h$-2$p$ ($n \times k l^2$) and so forth.

**4.6** Compute the number of 1$h$-1$p$ determinants in the case of $k$ inactive orbitals, $l$ virtual orbitals and a (2,2) CAS space for $M_S = 0$.

### *4.3.2 Difference Dedicated Configuration Interaction*

The majority of the excited determinants belong to the class of the 2$h$-2$p$ excitations. This class easily constitutes 90 % of the determinants in medium-sized molecules using basis sets of reasonable quality, and hence, the contribution to the correlation energy is extremely large. However, including this class of excitations in the configuration interaction expansions has only a small effect on the vertical excitation energies (that is, the relative energies of the different electronic states at a fixed geometry). Hence, this differential effect can be neglected in the calculation of the relative energies of the spin states needed to extract $J$, the magnetic coupling parameter of the Heisenberg Hamiltonian, and various other electronic structure parameters. The elimination of the 2$h$-2$p$ determinants leads to a drastic shortening of the configuration interaction expansion and widens the field of applicability of variational wave function based methods. The resulting variant of MRCI is generally known as the difference dedicated configuration interaction (DDCI) [12], which provides accurate vertical energy differences but cannot be used to compare total energies at different geometries.

**4.7** Make a rough estimate of the total number of determinants in the MR-CISD wave function for a system with 74 electrons, 154 orbitals and a CAS(2,2)CI reference wave function. Calculate the percentage of $2h$-$2p$ excitations in the MR-CISD wave function (neglect the $1h$, $1p$, $1h$-$1p$, $2h$ and $2p$ excitations, they give rise to a very small number of determinants).

The justification for eliminating the $2h$-$2p$ determinants relies on second-order perturbation theory in its quasi-degenerate formulation as exposed in Chap. 1. Although it can be done for an arbitrary number of unpaired electrons, we will elaborate the 2-electrons/2-orbitals case for simplicity. The model space is spanned by the neutral and ionic determinants

$$\Phi_I = \{|h\bar{h}a\bar{b}|, |h\bar{h}b\bar{a}|, |h\bar{h}a\bar{a}|, |h\bar{h}b\bar{b}|\} \tag{4.31}$$

where $h$ is one of the inactive orbitals, doubly occupied in all determinants of the model space. The lowest two eigenstates of the model space are the singlet and triplet spin functions whose energy difference is related to $J$. However, before diagonalizing we will first evaluate the effect of the $2h$-$2p$ external determinants on the matrix elements between the determinants of the model space with QDPT. First, we take a look at the off-diagonal elements and calculate the second-order contributions of $\Phi_R = |p\bar{p}a\bar{b}|$ and $\Phi_S = |p\bar{p}b\bar{a}|$ to the *dressed* matrix element of $\Phi_I = |h\bar{h}a\bar{b}|$ and $\Phi_J = |h\bar{h}b\bar{a}|$ according to the expression given in Eq. 1.86. The $2h$-$2p$ determinant $\Phi_R$ is obtained by making a double replacement in $\Phi_I$, exciting the electrons in $h$ to the unoccupied orbitals $p$ and $\Phi_S$ arises from $\Phi_J$ in an analogous way. The contributions to the effective matrix element are

$$\Phi_R\text{:} \quad \frac{\langle h\bar{h}a\bar{b}|\hat{V}|p\bar{p}a\bar{b}\rangle\langle p\bar{p}a\bar{b}|\hat{V}|h\bar{h}b\bar{a}\rangle}{E_J - E_R} \tag{4.32a}$$

$$\Phi_S\text{:} \quad \frac{\langle h\bar{h}a\bar{b}|\hat{V}|p\bar{p}b\bar{a}\rangle\langle p\bar{p}b\bar{a}|\hat{V}|h\bar{h}b\bar{a}\rangle}{E_J - E_S} \tag{4.32b}$$

For the contribution of $\Phi_R$, the second matrix element in the numerator is zero because the determinants on the left and the right of the operator have more than two different columns, and the same occurs for the first matrix element in the $\Phi_S$ contribution. This eliminates any second-order perturbation contribution from the $2h$-$2p$ determinants to the off-diagonal elements of the model space.

**4.8** Write down the second-order contribution of $\Phi_Q$ to $\langle \Phi_I|\hat{H}^{eff}|\Phi_L\rangle$, where $\Phi_Q$ arises from a double excitation from orbital $h$ to orbital $p$ acting on the ionic determinant $\Phi_L = |h\bar{h}b\bar{b}|$. Argue that this contribution is equal to zero.

On the contrary, the diagonal elements do have a contribution from the $2h$-$2p$ excitations. Continuing with the external determinants $\Phi_R$ and $\Phi_S$, it is easily shown that the former only contributes to $\langle \Phi_I | \hat{H}^{eff} | \Phi_I \rangle$ and the latter to $\langle \Phi_J | \hat{H}^{eff} | \Phi_J \rangle$

$$\Phi_R: \quad \frac{|\langle h\bar{h}a\bar{b}|\hat{V}|p\bar{p}a\bar{b}\rangle|^2}{E_I - E_R} \neq 0 \qquad \frac{|\langle h\bar{h}b\bar{a}|\hat{V}|p\bar{p}a\bar{b}\rangle|^2}{E_J - E_R} = 0 \tag{4.33a}$$

$$\Phi_S: \quad \frac{|\langle h\bar{h}a\bar{b}|\hat{V}|p\bar{p}b\bar{a}\rangle|^2}{E_I - E_S} = 0 \qquad \frac{|\langle h\bar{h}b\bar{a}|\hat{V}|p\bar{p}b\bar{a}\rangle|^2}{E_J - E_S} \neq 0 \tag{4.33b}$$

Both non-zero integrals are identical and through the Slater–Condon rules we arrive at the following second-order contribution of $\Phi_R$ and $\Phi_S$ to the diagonal elements $\langle \Phi_I | \hat{H}^{eff} | \Phi_I \rangle$ and $\langle \Phi_J | \hat{H}^{eff} | \Phi_J \rangle$

$$\frac{|\langle pp|\frac{1-\hat{P}_{12}}{r_{12}}|hh\rangle|^2}{2\varepsilon_h - 2\varepsilon_p} \tag{4.34}$$

where the denominator is obtained by assuming the Møller–Plesset division for $\hat{H} = \hat{H}^{(0)} + \hat{V}$. In the general case the contribution of all the $2h$-$2p$ determinants to the diagonal elements is given by

$$\sum_{h,h'} \sum_{p,p'} \frac{|\langle pp'|\frac{1-\hat{P}_{12}}{r_{12}}|hh'\rangle|^2}{\varepsilon_h + \varepsilon_{h'} - \varepsilon_p - \varepsilon_{p'}} \tag{4.35}$$

The summation only involves integrals that depend on the inactive ($h$, $h'$) and virtual ($p$, $p'$) orbitals, and hence, is exactly the same for all the diagonal elements in the model space. This uniform shift of the diagonal elements does not affect the energy differences of the eigenstates of the model space and in combination with the zero contribution to the off-diagonal elements, this shows that the $2h$-$2p$ determinants can be skipped in the CI expansion of the wave function. Note that this argument is based on second-order perturbation theory, the inclusion of higher-order interactions gives rise to small contributions and strictly speaking the mutual interaction between the $2h$-$2p$ determinants could affect the energy differences.

**4.9** Consider a (non-degenerate) model space with neutral and ionic determinants. (a) Show that the $2h$-$1p$ determinant $\Phi_R = |a\bar{a}p\bar{b}|$ introduces non-zero off-diagonal elements between the ionic and neutral determinants of the model space. (b) Are the diagonal elements of the model space shifted uniformly by $\Phi_R$?

The number of external determinants can even be more reduced when the model space is reduced to the neutral determinants $\Phi_I = \{|h\bar{h}a\bar{b}|, |h\bar{h}b\bar{a}|\}$. Under these

circumstances, the list of determinants that do not affect the energy difference of the two states contained by the model space can be extended with the $2h$-$1p$ and $1h$-$2p$ classes. Taking as an example $\Phi_R = |a\bar{a}p\bar{b}|$ and $\Phi_S = |b\bar{b}p\bar{a}|$ ($2h$-$1p$ determinant generated from $\Phi_I$ and $\Phi_J$, respectively), the same reasoning will be followed as above. In the first place it is easily seen that the second-order contribution to the off-diagonal elements is zero

$$\Phi_R\text{:}\quad \frac{\langle h\bar{h}a\bar{b}|\hat{V}|a\bar{a}p\bar{b}\rangle\langle a\bar{a}p\bar{b}|\hat{V}|h\bar{h}b\bar{a}\rangle}{E_J - E_R} = 0 \tag{4.36a}$$

$$\Phi_S\text{:}\quad \frac{\langle h\bar{h}a\bar{b}|\hat{V}|b\bar{b}p\bar{a}\rangle\langle b\bar{b}p\bar{a}|\hat{V}|h\bar{h}b\bar{a}\rangle}{E_J - E_S} = 0 \tag{4.36b}$$

The first integral in the numerator of the $\Phi_R$ contribution is non-zero because the determinants in the *bra* and the *ket* only differ by two columns, but $|a\bar{a}p\bar{b}|$ differs at three places from $|h\bar{h}b\bar{a}|$, and hence, leads to a zero contribution. The same holds for $\Phi_S$. At first sight, the contribution to the diagonal elements of the model space may seem non-uniform:

$$\Phi_R\text{:}\quad \frac{|\langle h\bar{h}a\bar{b}|\hat{V}|a\bar{a}p\bar{b}\rangle|^2}{E_I - E_R} \neq 0 \qquad \frac{|\langle h\bar{h}b\bar{a}|\hat{V}|a\bar{a}p\bar{b}\rangle|^2}{E_J - E_R} = 0 \tag{4.37a}$$

$$\Phi_S\text{:}\quad \frac{|\langle h\bar{h}a\bar{b}|\hat{V}|b\bar{b}p\bar{a}\rangle|^2}{E_I - E_S} = 0 \qquad \frac{|\langle h\bar{h}b\bar{a}|\hat{V}|b\bar{b}p\bar{a}\rangle|^2}{E_J - E_S} \neq 0 \tag{4.37b}$$

At difference with the $2h$-$2p$ determinants discussed above, the two non-zero integrals are not necessarily equal in this case. However, the effect of $\Phi'_R = |a\bar{a}b\bar{p}|$ and $\Phi'_S = |b\bar{b}a\bar{p}|$ exactly compensates this disequilibrium:

$$\Phi'_R\text{:}\quad \frac{|\langle h\bar{h}a\bar{b}|\hat{V}|a\bar{a}b\bar{p}\rangle|^2}{E_I - E'_R} = 0 \qquad \frac{|\langle h\bar{h}b\bar{a}|\hat{V}|a\bar{a}b\bar{p}\rangle|^2}{E_J - E'_R} \neq 0 \tag{4.38a}$$

$$\Phi'_S\text{:}\quad \frac{|\langle h\bar{h}a\bar{b}|\hat{V}|b\bar{b}a\bar{p}\rangle|^2}{E_I - E'_S} \neq 0 \qquad \frac{|\langle h\bar{h}b\bar{a}|\hat{V}|b\bar{b}a\bar{p}\rangle|^2}{E_J - E'_S} = 0 \tag{4.38b}$$

The denominators in the non-zero contributions of $\Phi_R$ and $\Phi'_R$ are equal since $E_R = E'_R$, and $E_I = E_J$ in a degenerate model space. Furthermore, the integral $\langle h\bar{h}a\bar{b}|\hat{V}|a\bar{a}p\bar{b}\rangle$ in Eq. 4.37a is exactly the same as the integral $\langle h\bar{h}b\bar{a}|\hat{V}|a\bar{a}b\bar{p}\rangle$ of Eq. 4.38a

$$\begin{aligned}\langle h\bar{h}a\bar{b}|\hat{V}|a\bar{a}p\bar{b}\rangle = \langle h\bar{h}a\bar{b}|\hat{H}|a\bar{a}p\bar{b}\rangle = -\langle h\bar{h}a\bar{b}|\hat{H}|p\bar{a}a\bar{b}\rangle = \\ -\langle h\bar{h}|\frac{1-\hat{P}_{12}}{r_{12}}|p\bar{a}\rangle = \int \frac{h(1)h(2)p(1)a(2)}{r_{12}} d\tau_1 d\tau_2\end{aligned} \tag{4.39a}$$

$$\langle h\bar{h}b\bar{a}|\hat{V}|a\bar{a}b\bar{p}\rangle = \langle h\bar{h}b\bar{a}|\hat{H}|a\bar{a}b\bar{p}\rangle = -\langle h\bar{h}b\bar{a}|\hat{H}|a\bar{p}b\bar{a}\rangle =$$
$$-\langle h\bar{h}|\frac{1-\hat{P}_{12}}{r_{12}}|a\bar{p}\rangle = \int \frac{h(1)h(2)a(1)p(2)}{r_{12}} d\tau_1 d\tau_2 \qquad (4.39b)$$

The same reasoning holds for $\Phi_S$ and $\Phi'_S$ showing that taking into account the $2h$-$1p$ and $1h$-$2p$ excitations only causes a uniform shift of the diagonal matrix elements, and hence, they can be left out of the calculation of the energy difference between the states of the model space.

This variant of the difference dedicated CI is commonly known as DDCI2 and gives reasonable energy differences for systems with a moderate importance of the ionic determinants. This is specially interesting for the treatment of organic biradicals or TM complexes with weakly coupled spin moments. However, the DDCI2 energy difference becomes increasingly more approximate when the CAS reference wave function contains non-negligible contributions from non-degenerate determinants. In these cases, one necessarily has to rely on the more expensive DDCI procedure. Finally, the external space is sometimes even further reduced by eliminating also the $2h$ and $2p$ determinants from the CI. The resulting CAS+S or DDCI1 method can be used to obtain a first impression of the relative size of the parameters, but does normally not provide accurate answers. Moreover, one should be aware of the practical problem that the implementations of this variant in different computer programs do not consider exactly the same list of determinants.

### *4.3.3 Multireference Perturbation Theory*

As an alternative for the variational methods, one can also apply multireference perturbation theory (MRPT) to calculate magnetic interactions. In principle, this type of calculations makes it possible to treat larger systems with more unpaired electrons. Among the many different implementations, two schemes are especially popular in the field of magnetic interactions: CASPT2 [13] and NEVPT2 [14, 15], which will be shortly overviewed here.

The standard Møller–Plesset perturbation theory uses a single determinant reference wave function and defines the zeroth-order Hamiltonian as the sum of the Fock operators

$$\hat{H}_{MP}^{(0)} = \sum \hat{F}_i \qquad (4.40)$$

By Koopmans' theorem, the eigenvalues of the Fock operator applied on occupied orbitals are proportional to ionization potentials and the eigenvalues corresponding to unoccupied orbitals are related to the electron affinities. CASPT2 extends the applicability to multireference cases by defining an effective one-electron Fock-type operator as zeroth order Hamiltonian in the following way

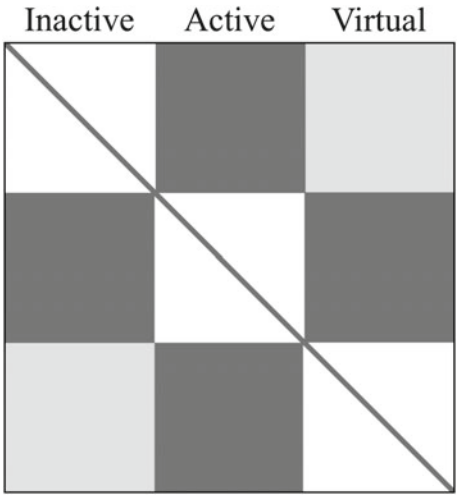


**Fig. 4.11** Structure of the $f$-matrix of $\hat{H}^{(0)}$ in CASPT2. The *dark grey* blocks have non-zero values, the *white blocks* are zero and the *light grey blocks* are zero when the orbitals are optimized for the state under study. For zero active orbitals only the diagonal elements survive and the Møller–Plesset definition of $\hat{H}^{(0)}$ emerges

$$\hat{H}^{(0)} = \sum_{rs\sigma} f_{rs\sigma} \hat{E}_{rs}; \text{ with } f_{rs\sigma} = -\langle 0|[[\hat{H}, \hat{a}^{\dagger}_{s\sigma}], \hat{a}_{r\sigma}]_{+}|0\rangle \tag{4.41}$$

where $|0\rangle$ is the CASSCF reference wave function and $\sigma$ a general index for the spin coordinates. This definition may appear complicated at first sight, but a closer look on the $f$-matrix learns that it is in fact a rather straightforward expression that reduces to the Møller–Plesset zeroth-order Hamiltonian in the limit of zero active orbitals.

$$f_{rs} = \langle 0|\hat{a}_r \hat{H} \hat{a}^{\dagger}_s|0\rangle - \langle 0|\hat{a}^{\dagger}_s \hat{H} \hat{a}_r|0\rangle - \langle 0|\hat{a}_r \hat{a}^{\dagger}_s \hat{H}|0\rangle + \langle 0|\hat{H} \hat{a}^{\dagger}_s \hat{a}_r|0\rangle \tag{4.42}$$

The structure of the matrix is schematically presented in Fig. 4.11. The inactive-virtual block of the matrix is given by

$$f_{hp} = \langle 0|\hat{a}_h \hat{H} \hat{a}^{\dagger}_p|0\rangle - \langle 0|\hat{a}^{\dagger}_p \hat{H} \hat{a}_h|0\rangle - \langle 0|\hat{a}_h \hat{a}^{\dagger}_p \hat{H}|0\rangle + \langle 0|\hat{H} \hat{a}^{\dagger}_p \hat{a}_h|0\rangle = 0 \tag{4.43}$$

where the first term is zero by $\langle 0|\hat{a}_h = \hat{a}^{\dagger}_h|0\rangle = 0$, since no particle can be created in an occupied orbital. The second and third term can be shown to be zero with an equivalent reasoning, while the fourth term is zero by the extended Brillouin theorem. The operator $\hat{a}^{\dagger}_p \hat{a}_h$ generates a singly excited configuration, which does not interact with the CASSCF wave function provided optimized orbitals are used. The diagonal elements of the inactive-inactive block are

$$f_{hh} = \langle 0|\hat{a}_h \hat{H} \hat{a}^{\dagger}_h|0\rangle - \langle 0|\hat{a}^{\dagger}_h \hat{H} \hat{a}_h|0\rangle - \langle 0|\hat{a}_h \hat{a}^{\dagger}_h \hat{H}|0\rangle + \langle 0|\hat{H} \hat{a}^{\dagger}_h \hat{a}_h|0\rangle = -IP_h \tag{4.44}$$

In this case, the first and third term are again zero for the same reason as exposed above. However, the operators in the second term annihilate an electron in the bra and the ket, which result in $\langle N-1|\hat{H}|N-1\rangle$, the energy of the ionized system.

The operator $\hat{a}_h^\dagger \hat{a}_h$ in the fourth term first annihilates an electron in orbital $h$ and subsequently creates it again in the same orbital. This leads to $\langle 0|\hat{H}|0\rangle$, the CASSCF energy of the $N$-electron system. The off-diagonal terms $f_{hh'}$ are all zero. Finally, we consider the virtual-virtual diagonal elements of $f$:

$$f_{pp} = \langle 0|\hat{a}_p \hat{H} \hat{a}_p^\dagger|0\rangle - \langle 0|\hat{a}_p^\dagger \hat{H} \hat{a}_p|0\rangle - \langle 0|\hat{a}_p \hat{a}_p^\dagger \hat{H}|0\rangle + \langle 0|\hat{H} \hat{a}_p^\dagger \hat{a}_p|0\rangle = -EA_p \quad (4.45)$$

The action of $\hat{a}_p$ on $|0\rangle$ (annihilation of an electron in an empty orbital) results in zeros for the second and fourth terms. $\langle 0|\hat{a}_p$ and $\hat{a}_p^\dagger|0\rangle$ generate an electron in orbital $p$ making the first term equal to the energy of the corresponding $(N+1)$-electron state. The third term is the energy of the CASSCF reference, and hence, the diagonal terms of the virtual-virtual block of $f$ are electron affinities. The off-diagonal elements $f_{pp'}$ are zero. Then it is readily seen that the CASPT2 $\hat{H}^{(0)}$ reduces to the Møller–Plesset Hamiltonian in the limit of zero active orbitals.

It is important to realize that the one-electron nature of $\hat{H}^{(0)}$ makes that the expectation values of the excited configurations $E_R^{(0)}$ appearing in the denominator of the corrections to the energy and wave function do not coincide with the expectation values of the real Hamiltonian $\hat{H}$. In some specific cases, it can happen that $E_R^{(0)}$ is very close to (or even smaller than) the expectation value of the ground state. Such *intruder* states may cause a break-down of the perturbation theory. CASPT2 implementations provide a pragmatic solution to this problem by the so-called level-shift technique, in which near-degeneracies are removed by adding an extra term to the denominator.

Although this approach often resolves the intruder state problem very efficiently, a methodologically more satisfying route is taken in the $n$-electron valence state second-order perturbation theory (NEVPT2). By including two-electron interactions in $\hat{H}^{(0)}$, this perturbative scheme does not suffer from the intruder state problem, except in some pathological cases. The zeroth-order Hamiltonian proposed by Dyall [16] reads

$$\hat{H}_D^{(0)} = \hat{H}_i + \hat{H}_v + C \quad (4.46)$$

where $\hat{H}_i$ is of one-electron nature and acts on the inactive and virtual orbitals

$$\hat{H}_i = \sum_h \varepsilon_h \hat{E}_{hh} + \sum_p \varepsilon_p \hat{E}_{pp} \quad (4.47)$$

$\hat{H}_v$ is a two-electron operator but is restricted to the active space

$$\hat{H}_v = \sum_{a,b} h_{ab}^{eff} \hat{E}_{ab} + \frac{1}{2} \sum_{a,b,c,d} \langle ab|\frac{1-\hat{P}_{12}}{r_{12}}|cd\rangle \left(\hat{E}_{ac}\hat{E}_{bd} - \delta_{bc}\hat{E}_{ad}\right) \quad (4.48)$$

and $C$ is an appropriate constant shift to ensure that $\hat{H}_D^{(0)}$ is equivalent to the full Hamiltonian in the active part.

**Contracted versus uncontracted**: The simplest way to define the first-order wave function is to apply single and double excitation operators on all the determinants (or CSFs) of the reference wave function.

$$\psi^{(1)} = \sum_I \sum_{rstu} c_{I,rstu} \hat{E}_{rs} \hat{E}_{tu} \Phi_I \tag{4.49}$$

The second-order correction to the energy is relatively straightforward to evaluate, but the number of terms in the summation rapidly becomes very large, especially for large reference wave functions. A second approach is to apply excitation operators not on the individual determinants of CSFs of the reference space, but on the reference wave function as a whole.

$$\psi^{(1)} = \sum_{rstu} c_{rstu} \hat{E}_{rs} \hat{E}_{tu} \psi^{(0)} \tag{4.50}$$

This approach generates much less terms since the external determinants appear as *contracted* sums in the first-order wave function. Moreover, the dimension of the external space does not grow as fast with the size of $\psi^{(1)}$ as in the uncontracted way of generating $\psi^{(1)}$. On the other hand, the calculation of the second-order correction to the energy relies on significantly more complicated expressions but once programmed this is just a minor issue compared to the limited length of $\psi^{(1)}$.

The differences between the contracted and uncontracted procedure are best illustrated by giving two examples with a very simple reference wave function: $\psi^{(0)} = \lambda|h\bar{h}a\bar{a}b| + \mu|h\bar{h}ab\bar{b}|$. In the first place, we will apply the single excitation operator involving the occupied orbital $h$ and the unoccupied orbitals $p$ and $p'$. The uncontracted wave function reads

$$\begin{aligned}\psi^{(1)} = {} & c_1|\bar{h}a\bar{a}bp| + c_2|ha\bar{a}b\bar{p}| + c_3|\bar{h}a\bar{a}bp'| + c_4|ha\bar{a}b\bar{p}'| \\ & + c_5|\bar{h}ab\bar{b}p| + c_6|hab\bar{b}\bar{p}| + c_7|\bar{h}ab\bar{b}p'| + c_8|hab\bar{b}\bar{p}'|\end{aligned} \tag{4.51}$$

and in the contracted formalism, the following function is generated

$$\begin{aligned}\psi^{(1)} = {} & c_1\{\lambda|\bar{h}a\bar{a}bp| + \mu|\bar{h}ab\bar{b}p|\} + c_2\{\lambda|ha\bar{a}b\bar{p}| + \mu|hab\bar{b}\bar{p}|\} \\ & + c_3\{\lambda|\bar{h}a\bar{a}bp'| + \mu|\bar{h}ab\bar{b}p'|\} + c_4\{\lambda|ha\bar{a}b\bar{p}'| + \mu|hab\bar{b}\bar{p}'|\}\end{aligned} \tag{4.52}$$

The uncontracted first-order correction has eight different coefficients to be determined, while the contracted variant generates the same determinants with only four different coefficients. The fact that the external determinants are weighted by the coefficients of the reference wave function does only slightly influence the final result. The second example applies the single excitation operator involving the active orbitals $a$ and $b$, and the virtual orbital $p$. Again, the uncontracted algorithm generates

a list of all five possible excited determinants

$$\psi^{(1)} = c_1|\bar{a}bp| + c_2|ab\bar{p}| + c_3|a\bar{a}p| + c_4|b\bar{b}p| + c_5|a\bar{b}p| \tag{4.53}$$

where the $h\bar{h}$-part has been omitted for simplicity. The contracted wave function is shorter:

$$\psi^{(1)} = c_1\{\lambda|\bar{a}bp| + \mu|b\bar{b}p|\} + c_2\lambda|ab\bar{p}| + c_3\{\lambda|a\bar{a}p| + \mu|a\bar{b}p|\} + c_4\mu|ab\bar{p}| \tag{4.54}$$

Since the determinants of the second and fourth term are the same, the wave function presents a linear dependence, which should be removed and further reduces the number of coefficients.

The contraction written in Eq. 4.50 is used in CASPT2 and in the *partially-contracted* variant of NEVPT2. The latter method is also available in a *strongly-contracted* variant of NEVPT2, in which the contracted external functions are grouped together depending on the number of electrons added or removed from the active space. In this way a reduced set of orthogonal external functions is generated.

### *4.3.4 Spin Unrestricted Methods*

The observation that except for the state of maximum multiplicity, spin states cannot be rigorously represented with a single determinant makes it very interesting to look at the possibility to study magnetic interactions in a spin unrestricted setting using a single determinant description of the spin states. We will start with the spatially symmetric 2-electron/2-orbital case and afterwards generalize for systems with more unpaired electrons.

The most widely applied approximation to extract $J$ within a single determinant description of the spin states is the so-called *Broken Symmetry* approach which uses two determinants:

$$\Phi_{BS} = |\phi_1\bar{\phi}_2| \qquad \Phi_{HS} = |\phi_1\phi_2| \tag{4.55}$$

where the closed-shell orbitals have been omitted for convenience. The $\hat{S}^2$ expectation value of $\Phi_{HS}$ is not exactly equal to 2 since the closed shell spin orbitals appear in pairs with slightly different spatial orbitals. However in most cases it is close to 2 and is generally considered as a good approximation to the triplet state obtained in a spin-restricted setting.

$$\Phi_{HS} \approx \Phi_T \tag{4.56}$$

$$E_{HS} = \langle\Phi_{HS}|\hat{H}|\Phi_{HS}\rangle \approx E_T \tag{4.57}$$

$$\langle\hat{S}^2\rangle_{HS} = \langle\Phi_{HS}|\hat{S}^2|\Phi_{HS}\rangle \approx 2 \tag{4.58}$$

One the other hand, the $\hat{S}^2$ expectation value of $\Phi_{BS}$ is neither close to zero (singlet) nor to two (triplet), but rather somewhere in between. It is therefore a logical step to approximate the broken symmetry determinant as a linear combination of the spin-restricted singlet and triplet states [17]:

$$|\Phi_{BS}\rangle = \lambda|\Phi_S\rangle + \mu|\Phi_T\rangle \qquad \text{with} \quad \lambda^2 + \mu^2 = 1 \tag{4.59}$$

with the following energy and $\hat{S}^2$ expectation value

$$E_{BS} = \langle \lambda\Phi_S + \mu\Phi_T|\hat{H}|\lambda\Phi_S + \mu\Phi_T\rangle = \lambda^2 E_S + \mu^2 E_T \tag{4.60}$$

$$\langle\hat{S}^2\rangle_{BS} = \lambda^2\langle\Phi_S|\hat{S}^2|\Phi_S\rangle + \mu^2\langle\Phi_T|\hat{S}^2|\Phi_T\rangle = 2\mu^2 \tag{4.61}$$

After substituting $\mu^2 = 1 - \lambda^2$ from the normalization condition in Eq. 4.61, we obtain

$$\lambda^2 = 1 - \frac{\langle\hat{S}^2\rangle_{BS}}{2} \qquad \text{and} \quad \mu^2 = \frac{\langle\hat{S}^2\rangle_{BS}}{2} \tag{4.62}$$

which can be substituted in the energy expression of the BS determinant given in Eq. 4.60

$$E_{BS} = \left(1 - \frac{\langle\hat{S}^2\rangle_{BS}}{2}\right)E_S + \frac{\langle\hat{S}^2\rangle_{BS}}{2}E_T \tag{4.63}$$

The energy difference of the BS and HS determinants now reads

$$\begin{aligned} E_{BS} - E_{HS} &= E_S - \frac{\langle\hat{S}^2\rangle_{BS}}{2}(E_S - E_T) - E_T \\ &= \left(1 - \frac{\langle\hat{S}^2\rangle_{BS}}{2}\right)(E_S - E_T) \\ &= \frac{2 - \langle\hat{S}^2\rangle_{BS}}{2}(E_S - E_T) \end{aligned} \tag{4.64}$$

which leads to the final expression of the magnetic coupling parameter $J$ as function of the energies of the spin-unrestricted HS and BS determinants

$$J = E_S - E_T = \frac{2(E_{BS} - E_{HS})}{2 - \langle\hat{S}^2\rangle_{BS}} \tag{4.65}$$

This is not the only expression used to relate the energy of the two determinants with the singlet-triplet energy difference. Under the assumption that the spin polarization in the closed shell orbitals is small enough to ensure their orthogonality, one

can express the energy difference as function of the overlap of the magnetic orbitals. From Eq. 1.27 we can calculate $\langle \hat{S}^2 \rangle_{BS}$

$$\begin{aligned}\langle \phi_1\overline{\phi}_2|\hat{S}^2|\phi_1\overline{\phi}_2\rangle &= \langle \phi_1\overline{\phi}_2|\phi_1\overline{\phi}_2 + \overline{\phi}_1\phi_2\rangle = \langle \phi_1\overline{\phi}_2|\phi_1\overline{\phi}_2 - \phi_2\overline{\phi}_1\rangle \\ &= 1 - \langle \phi_1|\phi_2\rangle^2 \end{aligned} \tag{4.66}$$

The substitution of this expression in Eq. 4.65 leads to

$$J = E_S - E_T = \frac{2(E_{BS} - E_{HS})}{1 + \langle \phi_1|\phi_2\rangle^2} \tag{4.67}$$

which in the weak overlap limit evolves to

$$J = 2(E_{BS} - E_{HS}) \tag{4.68}$$

and in the strong overlap limit to

$$J = E_{BS} - E_{HS} \tag{4.69}$$

Note that in the latter case the overlap $\langle \phi_1|\phi_2\rangle$ tends to one, which means that $\phi_1$ becomes equal to $\phi_2$ and $\Phi_{BS} = |\phi_1\overline{\phi}_1|$ represents a closed shell singlet state.

Expression 4.67 can be rewritten in terms of spin densities to avoid the less generally available overlap of the magnetic orbitals [18]. The simplest way to do this is to express the non-orthogonal magnetic orbitals $\phi_1$ and $\phi_2$ in the local orthogonal orbitals $\psi_1$ and $\psi_2$:

$$|\Phi_{BS}\rangle = |\phi_1\overline{\phi}_2\rangle = |(\lambda\psi_1 + \mu\psi_2)(\mu\overline{\psi}_1 + \lambda\overline{\psi}_2)\rangle \tag{4.70}$$

with $\langle \phi_1|\phi_1\rangle = \langle \phi_2|\phi_2\rangle = \lambda^2 + \mu^2 = 1$ and $\langle \phi_1|\phi_2\rangle = 2\lambda\mu$. The $\alpha$ and $\beta$ spin densities arise from $\phi_1$ and $\phi_2$, respectively, and are equal to $\lambda^2$ and $\mu^2$ for site 1. From this the total spin density can be obtained

$$\left.\begin{aligned}\rho_1^\alpha &= \lambda^2 \\ \rho_1^\beta &= \mu^2\end{aligned}\right\} \quad \Rightarrow \rho_1^{\alpha-\beta} = \lambda^2 - \mu^2 \overset{\lambda^2+\mu^2=1}{\Longrightarrow} \left\{\begin{aligned}2\lambda^2 &= 1 + \rho_1^{\alpha-\beta} \\ 2\mu^2 &= 1 - \rho_1^{\alpha-\beta}\end{aligned}\right. \tag{4.71}$$

Now the relation with $\langle \phi_1|\phi_2\rangle$ in Eq. 4.67 is easily made

$$\langle \phi_1|\phi_2\rangle^2 = 4\lambda^2\mu^2 = (1 + \rho_1^{\alpha-\beta})(1 - \rho_1^{\alpha-\beta}) = 1 - (\rho_1^{\alpha-\beta})^2 = 1 - (\rho_1^{BS})^2 \tag{4.72}$$

Note that this equation assumes that all the spin density is localized on the magnetic centers.

With a slightly more elaborate derivation one can also handle cases with an important delocalization of the spin density onto the ligands [19]. The magnetic orbitals are written as a linear combination of three nonorthogonal basis functions

$$\phi_1 = \lambda\chi_1 + \mu\chi_2 + \nu\chi_3 \qquad \phi_2 = \mu\chi_1 + \lambda\chi_2 + \nu\chi_4 \tag{4.73}$$

with $\langle\chi_i|\chi_j\rangle \neq 0$, $\langle\chi_i|\chi_i\rangle = 1$ and $\lambda \gg \mu, \nu$. The basis functions $\chi_1$ and $\chi_2$ are centered on the magnetic site 1 and 2, respectively. The other two functions are ligand orbitals around site 1 ($\chi_3$) and site 2 ($\chi_4$). Furthermore, it holds that $\langle\chi_1|\chi_4\rangle = \langle\chi_2|\chi_3\rangle \ll \langle\chi_1|\chi_3\rangle = \langle\chi_2|\chi_4\rangle$ in a centro-symmetric system. The overlap of the two magnetic orbitals is

$$\begin{aligned}\langle\phi_1|\phi_2\rangle = {} & 2\lambda\mu + \nu^2\langle\chi_3|\chi_4\rangle + (\lambda^2 + \mu^2)\langle\chi_1|\chi_2\rangle \\ & + 2\lambda\nu\langle\chi_1|\chi_4\rangle + 2\mu\nu\langle\chi_1|\chi_3\rangle\end{aligned} \tag{4.74}$$

Many terms can be neglected in this expression. The terms with $\mu^2$, $\nu^2$ or $\mu\nu$ are small because these coefficients are much smaller than $\lambda$. Being located in different parts of the complex, the overlap integrals $\langle\chi_1|\chi_4\rangle$ and $\langle\chi_1|\chi_2\rangle$ are also expected to be small. This makes that the overlap of the magnetic orbitals can be roughly approximated by $2\lambda\mu$. The spin density on site 1 can be determined using the Mulliken population reasoning. The contribution due to $\phi_1$ and $\phi_2$ are

$$\phi_1 \text{ contribution:} \qquad \lambda^2 + \frac{1}{2}(2\lambda\mu\langle\chi_1|\chi_2\rangle + 2\lambda\nu\langle\chi_1|\chi_3\rangle) \tag{4.75}$$

$$\phi_2 \text{ contribution:} \qquad \mu^2 + \frac{1}{2}(2\lambda\mu\langle\chi_1|\chi_2\rangle + 2\mu\nu\langle\chi_1|\chi_4\rangle) \tag{4.76}$$

which reduce to $\lambda^2$ and $\mu^2$ if we apply the same approximations as for the overlap of the magnetic orbitals. The spin density at the magnetic sites for $\Phi_{HS}$ and $\Phi_{BS}$ are given by

$$\rho_1^{HS} = \lambda^2 + \mu^2 \qquad \rho_1^{BS} = \lambda^2 - \mu^2 \tag{4.77}$$

Now it is easily derived that

$$(\rho_1^{HS})^2 - (\rho_1^{BS})^2 = 4\lambda^2\mu^2 = \langle\phi_1|\phi_2\rangle^2 \tag{4.78}$$

which can be used to replace the overlap integral in Eq. 4.67 with the more generally available spin populations. This expression is valid for centro-symmetric systems but improves the previous one by the fact that it is no longer implicit that the spin density in the HS state is entirely located on the magnetic center.

The extension of Eq. 4.65 to the general case of magnetic coupling between two centers with more than one unpaired electron is straightforward and follows the same logics. The spin-unrestricted HS determinant $\Phi_{HS}$ is assumed to be a good approximation to the spin eigenfunction of maximum multiplicity $\Phi_{S_{max}}$, and therefore,

$$\langle\hat{S}^2\rangle_{HS} = S_{max}(S_{max} + 1) \qquad E_{HS} = E_{S_{max}} \tag{4.79}$$

The broken symmetry determinant is written as a linear combination of the singlet $\Phi_S$ and the $S_{max}$ spin eigenfunctions.[2]

$$|\Phi_{BS}\rangle = \lambda|\Phi_S\rangle + \mu|\Phi_{S_{max}}\rangle = \lambda|\Phi_S\rangle + \mu|\Phi_{HS}\rangle \tag{4.80}$$

From the $\hat{S}^2$ expectation value

$$\langle\hat{S}^2\rangle_{BS} = \lambda^2\langle\Phi_S|\hat{S}^2|\Phi_S\rangle + \mu^2\langle\Phi_{HS}|\hat{S}^2|\Phi_{HS}\rangle = \langle\hat{S}^2\rangle_{HS}\mu^2 \tag{4.81}$$

one arrives at

$$E_{BS} = \lambda^2 E_S + \mu^2 E_{HS} = \left(1 - \frac{\langle\hat{S}^2\rangle_{BS}}{\langle\hat{S}^2\rangle_{HS}}\right)E_S + \frac{\langle\hat{S}^2\rangle_{BS}}{\langle\hat{S}^2\rangle_{HS}}E_{HS} \tag{4.82}$$

Then, the energy difference between $\Phi_{BS}$ and $\Phi_{HS}$ is given by

$$\begin{aligned} E_{BS} - E_{HS} &= E_S - \frac{\langle\hat{S}^2\rangle_{BS}}{\langle\hat{S}^2\rangle_{HS}}(E_S - E_{HS}) - E_{HS} \\ &= \frac{\langle\hat{S}^2\rangle_{HS} - \langle\hat{S}^2\rangle_{BS}}{\langle\hat{S}^2\rangle_{HS}}(E_S - E_{HS}) \qquad (4.83) \\ \Rightarrow E_S - E_{HS} &= \frac{\langle\hat{S}^2\rangle_{HS}(E_{BS} - E_{HS})}{\langle\hat{S}^2\rangle_{HS} - \langle\hat{S}^2\rangle_{BS}} \qquad (4.84) \end{aligned}$$

from which the expression for $J$ is directly derived

$$J = \frac{2(E_S - E_{HS})}{S_{max}(S_{max}+1)} = \frac{2(E_S - E_{HS})}{\langle\hat{S}^2\rangle_{HS}} = \frac{2(E_{BS} - E_{HS})}{\langle\hat{S}^2\rangle_{HS} - \langle\hat{S}^2\rangle_{BS}} \tag{4.85}$$

This is the famous Yamaguchi relation originally derived in the framework of unrestricted Hartree–Fock calculations [20], but later also widely applied in DFT calculations. In the limit of zero overlap of the magnetic orbitals, $\langle\hat{S}^2\rangle_{BS}$ becomes equal to $S_{max}$ and the following expression emerges

$$J = \frac{2(E_{BS} - E_{HS})}{S_{max}(S_{max}+1) - S_{max}} = \frac{2(E_{BS} - E_{HS})}{S_{max}^2} \tag{4.86}$$

derived earlier by Noodleman [21] and which reduces to Eq. 4.68 for two magnetic centers with S=1/2. On the other hand, $\langle\hat{S}^2\rangle_{BS}$ is zero in the strong overlap limit and $J$ relates to the energies of the HS and BS determinants as

[2]This is of course an approximation. There is no obvious reason to exclude the intermediate spin states from the linear combination.

$$J = \frac{2(E_{BS} - E_{HS})}{S_{max}(S_{max} + 1)} \tag{4.87}$$

which is the generalized form of Eq. 4.69. This expression is also used in DFT when the BS determinant is considered to be a good representation of the singlet (or lowest spin) state as proposed by Ruiz and co-workers [6, 19, 22]. These authors often replace the denominator by $2(2S_1S_2 + S_2)$ with $S_2 \geqslant S_1$ and $S_1 + S_2 = S_{max}$ to reflect situations with unequal spin moments on the two magnetic centers.

**4.10** Calculate the expectation value of $\hat{S}^2$ for $\Phi_1 = |\phi_1\phi_2\overline{\phi}_3\overline{\phi}_4|$ in the zero overlap limit: $\langle\phi_i|\phi_j\rangle = \delta_{ij}$.

### *4.3.5 Alternatives to the Broken Symmetry Approach*

The introduction of the broken symmetry determinant as representation of the low-spin coupled spin state not only provides (computational) chemists with a tool to calculate magnetic interactions with single determinant methods, it also makes a connection with the intuitive representations of spins with up- and downwards pointing arrows at each magnetic center. However, this representation does not lead to spin functions that are eigenfunctions of the total spin operator $\hat{S}^2$, as expected in a non-relativistic setting and explained in Chap. 1. From this point of view the broken symmetry approach is less satisfactory and there have been many attempts to design alternative approaches to calculate magnetic interactions with DFT to improve upon the shortcomings of the standard approach.

A natural starting point is to combine a multiconfigurational SCF approach to treat the static electron correlation[3] and DFT for the remaining (mainly dynamic) electron correlation. It is, however, not easy to design functionals that only take into account this latter part of the electron correlation and do not consider (part of) the static correlation. Despite many efforts, there seems no definitive solution to the double counting problem.

**Restricted ensemble Kohn–Sham DFT** Alternatively one can perform standard KS-DFT calculations on a collection of determinants with different occupations and take a weighted average of the individual energies to obtain an estimate of the multideterminantal situation. To avoid the independent calculation of several KS determinants, a generalization of this approach was proposed by Filatov and Shaik based on the coupling operator technique developed by Roothaan for restricted open-shell Hartree–Fock. This restricted open-shell Kohn–Sham (ROKS) approach was later extended to situations where fractional occupation numbers are not imposed by the

[3] In the case of magnetic interactions, the multideterminantal character of the $N$-electron states with $S < S_{max}$.

symmetry (as in atomic multiplets or ligand-field states in coordination complexes) but due to *accidental* (near-)degeneracies. This extended approach was named the restricted ensemble Kohn–Sham (REKS) method [23, 24]. An optimal set of Kohn–Sham orbitals and occupation numbers is obtained by a minimization procedure that always maintains the spin and spatial symmetry of the $N$-electron state under study.

The approach has been used to calculate the coupling of two localized spin moments in binuclear transition metal complexes and the singlet-triplet splitting in biradical systems, such as twisted ethylene. Rather reasonable values of the magnetic coupling parameters were obtained. In general, the couplings are slightly too small, which may be attributed to the lack of spin polarization. An important advantage of the method is the fact that geometries can be optimized for open-shell singlet states within the DFT framework.

**Spin-flip time-dependent DFT** The energy differences of the spin states involved in the magnetic interaction of two (or more) spin moments can be seen to some extent as vertical excitation energies, and hence, time-dependent DFT (or other linear response methods as equation of motions coupled cluster [25]) could in principle be used to determine the magnetic interaction between two spin moments. However, the standard implementation of TD-DFT only considers single, *spin-conserving* excitations, which prevents accounting for the multideterminantal character of the states with low-spin coupling [26]. Figure 4.12 shows the five determinants that are essential to describe the magnetic coupling in a two-electron/two-orbital problem. Using determinant $\Phi_1$, $\Phi_2$ or $\Phi_3$ as reference will not generate all five determinants in standard TD-DFT, while $\Phi_4$ and $\Phi_5$ lead to the same spin contamination problems as in the BS approach discussed above. The spin-flip formalism (originally developed in the framework of Hartree–Fock and coupled cluster, and later implemented for TD-DFT) offers an interesting solution to this shortcoming. The determinant with maximum $M_S$-value is taken as reference ($\Phi_1$ in Fig. 4.12) and all single excited determinants involving one spin-flip are generated from this. Within the space of the two-electron/two-orbital problem, this procedure generates the determinants $\Phi_2 \ldots \Phi_5$ of Fig. 4.12, and hence, gives access to the energy of the open-shell singlet within the TD-DFT framework without spin-contamination problems.

**Constrained DFT** The basic shortcomings of the BS approach can be summarized in two points. In the first place, the spin contamination, or the impossibility to represent the low-spin states with a single Kohn–Sham determinant. The second point is the fact that nearly all todays functionals tend to overestimate the delocalization of the spin density and overestimate the antiferromagnetic character of the coupling.


**Fig. 4.12** The reference determinant $\Phi_1$ and the four spin-flip determinants ($\Phi_2 \ldots \Phi_5$) generated in SF-TDDFT with a two-electron/two-orbital target space

Constrained DFT (C-DFT) remedies, at least partially, the latter by putting restrictions on the spatial distributions of the $\alpha$ and $\beta$ electrons [27]. Two fragments $p$ and $q$ are defined such that both include one magnetic center and the atoms around it. Subsequently, the density is optimized under the restrictions that $N_\alpha^p - N_\beta^p = M_S^p$ and $N_\alpha^q - N_\beta^q = M_S^q$, where $N_{\alpha,\beta}^{p,q}$ are the summed spin populations of the atoms in the fragments and $M_S^{p,q}$ the prefixed excess of $\alpha$ or $\beta$ electrons in each fragment. C-DFT results in less delocalized spin densities and therefore, in general, to smaller interaction parameters.

## Problems

**4.1** A master student wants to study the energy splitting $E_S - E_T$ in a planar $[Cu_2F_6]^{2-}$ model system, since experimental studies of similar di Cl-bridged $Cu^{II}$ dimers suggested that $E_S - E_T$ depends strongly on the Cu–Cl–Cu angle $\theta$. She performs RHF calculations on the triplet state in order to predict $E_S - E_T$ with the HTH model. She produces a Table of results, where the *gerade* and *ungerade* open shell orbitals are denoted 1 and 2, respectively.

| $\theta$ | $\frac{J_{11}+J_{22}}{2} - J_{12}$ [K] | $K_{12}$ [$E_h$] | $\varepsilon_1 - \varepsilon_2$ [$E_h$] |
|---|---|---|---|
| 85° | 24 | 0.4324 | −0.0078 |
| 90° | 20 | 0.4376 | −0.0025 |
| 95° | 22 | 0.4419 | 0.0034 |
| 100° | 26 | 0.4456 | 0.0094 |
| 105° | 32 | 0.4483 | 0.0150 |

Compute $J$ (in K) for $\theta = 85° \ldots 105°$ using the HTH model. Do you observe a strong dependence of the coupling on the angle? Can the same conclusions be drawn when only considering the orbital energies?

**4.2 Quantifying the counter-complementarity effect**. Standard optimization of the molecular orbitals of a magnetic complex with two magnetic centers bridged by two different ligands normally leads to magnetic orbitals with contributions on both ligands (as $\varphi_5$ and $\varphi_6$ in Fig. 4.9). This makes it very hard to quantify the counter-complementary effect of the two ligands. Design a computational strategy to determine quantitatively the reduction of the magnetic coupling through ligand 1 by the counter-complementary effect of ligand 2. Hint: Many quantum chemical programs can divide the whole system into fragments.

**4.3 Broken symmetry approach**. The magnetic coupling of three binuclear TM complexes has been studied with DFT. The following results were obtained for the HS and BS determinants. (a) Calculate the magnetic coupling parameter $J$ with the Yamaguchi equation (Eq. 4.85) and compare the outcomes to the alternative relations of Noodleman (Eq. 4.86) and Ruiz (Eq. 4.87).

| TM | Energy [$E_h$] | | $\langle \hat{S}^2 \rangle$ | |
|---|---|---|---|---|
| | $\Phi_{HS}$ | $\Phi_{BS}$ | $\Phi_{HS}$ | $\Phi_{BS}$ |
| $Cu^{2+}$ | −4061.7435920 | −4061.7442381 | 2.0035 | 0.9957 |
| $Ni^{2+}$ | −3797.4742498 | −3797.4767694 | 6.0083 | 1.9931 |
| $Mn^{2+}$ | −3082.7586297 | −3082.7630415 | 30.0086 | 4.9936 |

(b) Calculate $J$ in the Cu complex combining Eqs. 4.67 and 4.78 using $\rho^{\alpha-\beta}$ is 0.6864 and 0.6757 for HS and BS, respectively.

## References


1. O. Kahn, B. Briat, J. Chem. Soc., Faraday Trans. **2**(72), 268 (1976)
2. P.J. Hay, J.C. Thibeault, R.J. Hoffmann, J. Am. Chem. Soc. **97**, 4884 (1975)
3. H.M. McConnell, J. Chem. Phys. **39**, 1910 (1963)
4. M. Deumal, J.J. Novoa, M.J. Bearpark, P. Celani, M. Olivucci, M.A. Robb, J. Phys. Chem. A **102**, 8404 (1998)
5. J.J. Novoa, M. Deumal, Struct. Bond. **100**, 33 (2001)
6. E. Ruiz, P. Alemany, S. Alvarez, J. Cano, J. Am. Chem. Soc. **119**, 1297 (1997)
7. O. Kahn, *Molecular Magnetism* (VCH Publishers, New York, 1993)
8. J.P. Launay, M. Verdaguer, *Electrons in Molecules: From Basic Principles to Molecular Electronics* (Oxford University Press, Oxford, 2014)
9. O. Kahn, J. Galy, Y. Journaux, J. Jaud, I. Morgenstern-Badarau, J. Am. Chem. Soc. **104**, 2165 (1982)
10. R. Costa, A. Garcia, J. Ribas, T. Mallah, Y. Journaux, J. Sletten, X. Solans, V. Rodríguez, Inorg. Chem. **32**, 3733 (1993)
11. T. Helgaker, P. Jørgensen, J. Olsen, *Molecular Electronic-structure Theory* (Wiley, Chichester, 2000)
12. J. Miralles, O. Castell, R. Caballol, J.P. Malrieu, Chem. Phys. **172**, 33 (1993)
13. K. Andersson, P.Å. Malmqvist, B.O. Roos, J. Chem. Phys. **96**, 1218 (1992)
14. C. Angeli, R. Cimiraglia, S. Evangelisti, T. Leininger, J.P. Malrieu, J. Chem. Phys. **114**, 10252 (2001)
15. C. Angeli, R. Cimiraglia, J.P. Malrieu, J. Chem. Phys. **117**(20), 9138 (2002)
16. K.G. Dyall, J. Chem. Phys. **102**, 4909 (1995)
17. J.P. Malrieu, R. Caballol, C.J. Calzado, C. de Graaf, N. Guihéry, Chem. Rev. **114**, 429 (2014)
18. R. Caballol, O. Castell, F. Illas, I. de P.R. Moreira, J.P. Malrieu, J. Phys. Chem. A **101**(42), 7860 (1997)
19. E. Ruiz, J. Cano, S. Alvarez, P. Alemany, J. Comput. Chem. **20**(13), 1391 (1999)
20. K. Yamaguchi, H. Fukui, T. Fueno, Chem. Lett. **15**, 625 (1986)
21. L. Noodleman, J. Chem. Phys. **74**, 5737 (1981)
22. J.P. Perdew, A. Savin, K. Burke, Phys. Rev. A **51**(6), 4531 (1995)
23. M. Filatov, S. Shaik, Chem. Phys. Lett. **288**, 689 (1998)
24. M. Filatov, S. Shaik, Chem. Phys. Lett. **304**, 429 (1999)
25. A.I. Krylov, Chem. Phys. Lett. **350**, 522 (2001)
26. Y.A. Bernard, Y. Shao, A.I. Krylov, J. Chem. Phys. **136**, 204103 (2012)
27. B. Kaduk, T. Kowalczyk, T. Van Voorhis, Chem. Rev. **112**, 321 (2012)